Inorganic Chemistry

Article

pubs.acs.org/IC

Luminescence Modulations of Rhenium Tricarbonyl Complexes Induced by Structural Variations

Hélène C. Bertrand,*[,†,‡,§] Sylvain Clède,[†,‡,§] Régis Guillot,[∥] François Lambert,[†,‡,§] and Clotilde Policar[†,‡,§]

[†]Sorbonne Universités, UPMC Univ Paris 06, UMR 7203, Laboratoire des Biomolécules, F-75005 Paris, France

[‡]CNRS, UMR 7203, Laboratoire des Biomolécules, F-75005 Paris, France

[§]ENS, Département de Chimie, Laboratoire des Biomolécules, 24 rue Lhomond, 75005 Paris, France

[∥]Université Paris-Sud, ICMMO, UMR CNRS 8182, 91405 Orsay, France

Supporting Information

ABSTRACT: Octahedral d^6 low-spin Re(I) tricarbonyl complexes are of considerable interest as noninvasive imaging probes and have been deeply studied owing to their biological stability, low toxicity, large Stokes shifts, and long luminescence lifetimes. We reported recently the bimodal IR and luminescence imaging of a Re(I) tricarbonyl complex with a Pyta ligand (4-(2-pyridyl)-1,2,3-triazole) in cells and labeled such metal−carbonyl complexes SCoMPIs for single-core multimodal probes for imaging. Re(I) tricarbonyl complexes have unique photophysical properties allowing for their unequivocal detection in cells but also present some weaknesses such as a very low luminescence quantum yield in aqueous medium. Further optimizations would thus be desirable. We therefore developed new Re(I) tricarbonyl complexes prepared from different ancillary ligands. Complexes with benzothiadiazole−triazole ligands show interesting luminescent quantum yields in acetonitrile and may constitute valuable luminescent metal complexes in organic media. A series of complexes with bidentate 1-(2-quinolinyl)-1,2,3-triazole (Taquin) and 1-(2-pyridyl)-1,2,3-triazole (Tapy) ligands bearing various 4-substituted alkyl side chains has been designed and synthesized with efficient procedures. Their photophysical properties have been characterized in acetonitrile and in a H_2O/DMSO (98/2) mixture and compared with those of the parent Quinta- and Pyta-based complexes. Tapy complexes bearing long alkyl chains show impressive enhancement of their luminescent properties relative to the parent Pyta complex. Theoretical calculations have been performed to further characterize this new class of rhenium tricarbonyl complexes. Preliminary cellular imaging studies in MDA-MB231 breast cancer cells reveal a strong increase in the luminescence signal in cells incubated with the Tapy complex substituted with a C12 alkyl chain. This study points out the interesting potential of the Tapy ligand in coordination chemistry, which has been so far underexploited.

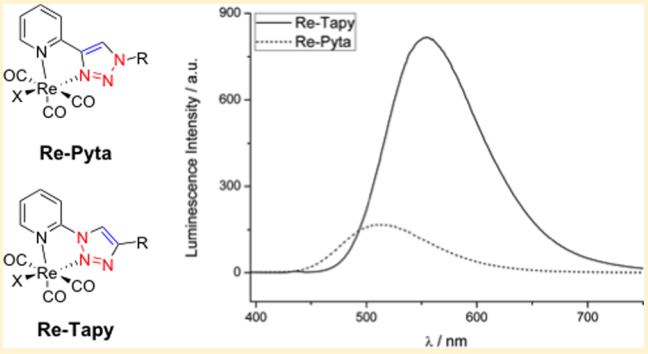

INTRODUCTION

Organometallic complexes have become of major interest as noninvasive imaging probes.[1] Among them, luminescent polypyridine-based transition-metal complexes have received considerable attention, with their photophysical properties being valuable for bioimaging.[2] In particular, octahedral d^6 low-spin Re(I) tricarbonyl complexes have been deeply studied owing to their biological stability, low toxicity, large Stokes shifts, and long luminescence lifetimes.[3] In this class of compounds, the photophysical properties of the complexes are closely dependent on the ligand. Originally developed with 2,2′-bipyridine derivatives, numerous Re(I) tricarbonyl complexes have been designed that incorporate other aromatic poly-azaheterocycles[2b,4] of easier synthetic access and functionalization. In that context the ligand 4-(2-pyridyl)-1,2,3-triazole (Pyta) has been widely used for the preparation of luminescent Re(I) complexes. Many functionalized derivatives have been developed with a pendant side chain of different chemical nature, an alkyl or aromatic group, or a functionalization suitable for further grafting on a biomolecule.[5] Our group recently reported the use of such metal−carbonyl complexes to couple infrared and luminescence detection in cells.[6] Indeed, a Re(I) tricarbonyl complex with a Pyta ligand enabled its multimodal imaging in cells. This bioimaging study is at the origin of the concept of a single-core multimodal probe for imaging (SCoMPI).[6] This has been successfully applied to the investigation of the cellular location of an estrogen derivative conjugate in breast cancer cells.[7]

Re(I) tricarbonyl complexes have unique photophysical properties allowing for their unequivocal detection in cells but present also some weaknesses such as a very low luminescence

Received: March 26, 2014
Published: June 6, 2014

   dx.doi.org/10.1021/ic5007007 | *Inorg. Chem.* 2014, 53, 6204−6223

quantum yield in aqueous medium (typically around 0.7%). Further optimizations would thus be desirable: a higher excitation wavelength would allow freeing images from cell autofluorescence and an increase in the quantum yield in aqueous medium would be beneficial. We therefore developed new Re(I) tricarbonyl complexes prepared from different ancillary ligands. We particularly focused on the 1-(2-pyridyl)-1,2,3-triazole ligand and derivatives with extended aromatic surfaces.[8] This ligand is called thereafter Tapy by analogy with Pyta, which is a regioisomer and only differs in the position of the bridge between the pyridine and the triazole rings. The coordination properties of such ligands have been surprisingly overlooked, and no example of rhenium tricarbonyl complexes incorporating such ligands in their coordination sphere has been found in the literature. We also developed complexes prepared from a Tapy analogue, labeled TaBTD, in which the pyridine ring was substituted with a benzothiadiazole unit.

We present here the synthesis and characterization of these new ligands along with their corresponding rhenium tricarbonyl complexes. Their photophysical properties have been studied in detail, and theoretical studies were performed to further characterize some of the complexes described. A rhenium tricarbonyl complex with a Tapy ligand bearing a C12 alkyl chain showed an unexpectedly high increase in luminescence intensity and quantum yield in aqueous solution in comparison to the corresponding Pyta complex. Preliminary imaging studies show a strong luminescence intensity enhancement in incubated breast cancer MDA-MB-231 cells.

EXPERIMENTAL SECTION

Chemistry. *General Considerations.* ^{1}H and ^{13}C NMR spectra were recorded on a Bruker Avance 300 or 600 spectrometer using solvent residuals as internal references. The following abbreviations are used: singlet (s), doublet (d), doublet of doublets (dd), triplet (t), doublet of triplets (td), quintuplet (quint), sextuplet (sext), and multiplet (m). Mass spectrometry services were performed at the ICMMO (Université Paris Sud, Orsay, France) and at UMR7201 (Université Pierre et Marie Curie). The following abbreviations are used: MS (mass spectrometry), HRMS (high resolution mass spectrometry), electrospray (ESI), time-of-flight (TOF). TLC analysis was carried out on silica gel (Merck 60F-254) with visualization at 254 and 366 nm. Preparative flash chromatography was carried out with Merck silica gel (Si 60, 40−63 μm). Reagents and chemicals were purchased from Sigma-Aldrich, Alfa Aesar, or Strem Chemicals. Dry solvents (dichloromethane (CH_2Cl_2 or DCM), toluene, tetrahydrofuran (THF), and dimethylformamide (DMF)) were purchased from Sigma and used without further purification. UV−vis absorption spectra were recorded on a Varian Cary 300 Bio spectrophotometer, luminescence emission spectra on a Jasco FP-8300 spectrofluorometer, and IR spectra on a Perkin-Elmer Spectrum 100 FT-IR spectrometer. Analytical HPLC measurements were run on a Dionex Ultimate 3000 instrument using C8A or C18A ACE columns. Though no problem was encountered in the handling of any of the azides used, these compounds are potentially explosive and should thus be manipulated with caution. 2-Methyl-4-(2′-quinolyl)-but-3-yn-2-ol (**9**) and 2-ethynylquinoline (**10**) were synthesized according to published procedures.[9]

*Tetrazolo[1,5-a]quinoxaline (**1**).* 2-Chloroquinoxaline (100.0 mg, 0.607 mmol, 1.0 equiv) was dissolved in DMF (2.6 mL) and NaN_3 (237.0 mg, 3.65 mmol, 6.0 equiv) was added. The mixture was stirred at 110 °C under N_2 for 24 h. The mixture was diluted with H_2O and extracted twice with EtOAc. The organic phase was washed with saturated brine, dried over $MgSO_4$, filtered, and evaporated to afford tetrazolo[1,5-*a*]quinoxaline (**1**) as a pale orange solid (98.0 mg, 94% chemical yield). The analytical data were in accordance with those in the literature.[8,10]

^{1}H NMR (300 MHz, $CDCl_3$): δ (ppm) 9.60 (s, 1H), 8.68 (dd, *J* = 1.2, 8.1 Hz, 1H), 8.36 (dd, *J* = 1.5, 8.1 Hz, 1H), 7.97 (td, *J* = 1.5, 8.1 Hz, 1H), 7.91 (td, *J* = 1.5, 8.1 Hz, 1H). ^{13}C NMR (75 MHz, $CDCl_3$): δ (ppm) 142.5, 141.3, 136.9, 131.9, 130.9, 130.0, 125.1, 116.5.

*Tetrazolo[1,5-a]quinoline (**2**).* 2-Chloroquinoline (500.0 mg, 3.06 mmol, 1.0 equiv) was dissolved in a DMF/H_2O 13/5 mixture (18 mL), and NaN_3 (1.19 g, 18.34 mmol, 6.0 equiv) was added. The mixture was stirred at 85 °C under Ar for 3 days. The mixture was diluted with H_2O and extracted twice with EtOAc. The organic phase was washed with H_2O, dried over $MgSO_4$, filtered, and evaporated to afford tetrazolo-[1,5-*a*]quinoline (**2**) as a white solid (480.0 mg, 92% chemical yield). The analytical data were in accordance with those in the literature.[8,11]

^{1}H NMR (300 MHz, $CDCl_3$): δ (ppm) 8.70 (d, *J* = 8.4 Hz, 1H), 7.98 (m, 2H), 7.88 (m, 2H), 7.72 (td, *J* = 1.2 Hz, 8.4 Hz, 1H). ^{13}C NMR (75 MHz, $CDCl_3$): δ (ppm) 133.4, 131.4, 131.0, 129.1, 128.1, 124.0, 117.0, 112.8.

General Procedure A for $(CuOTf)_2{\cdot}C_6H_6$-Catalyzed CuAAC Click Reaction. A vial was charged with the tetrazolo or azido derivative (1.0 equiv) and copper(I) trifluoromethanesulfonate benzene complex (10 mol %). After three vacuum/N_2 purges, dry toluene (1.0 mL/0.15 mmol) was added under an inert atmosphere, followed by the alkyne derivative (1.1 equiv). The vial was closed with a screwed cap and secured by Teflon tape. The reaction mixture was stirred at 100 °C. The reaction mixture was then diluted with EtOAc or DCM and H_2O. The organic phase was decanted out, washed with water and saturated brine, dried over Na_2SO_4, filtered, and evaporated. The residue was purified by column chromatography on silica gel to afford the desired compound.

*2-(4-Octyl-1H-1,2,3-triazol-1-yl)quinoxaline (**3**).* This compound was obtained following the general procedure A starting from tetrazolo[1,5-*a*]quinoxaline (**1**; 26.4 mg, 0.15 mmol, 1.0 equiv) and 1-decyne (30.7 μL, 0.17 mmol, 1.1 equiv) after column chromatography on silica gel (eluent cyclohexane/EtOAc 7/3) as a pale yellow solid (26.0 mg, 55% chemical yield).

R_f (cyclohexane/EtOAc 7/3) = 0.61. ^{1}H NMR (300 MHz, $CDCl_3$): δ (ppm) 9.81 (s, 1H), 8.46 (s, 1H), 8.17 (m, 1H), 8.03 (m, 1H), 7.81 (m, 2H), 2.85 (td, *J* = 0.8, 7.5 Hz, 2H), 1.78 (quint, *J* = 7.5 Hz, 2H), 1.45−1.25 (m, 10H), 0.87 (m, 3H). ^{13}C NMR (75 MHz, $CDCl_3$): δ (ppm) 149.7, 143.3, 142.3, 140.2, 138.1, 131.6, 130.3, 129.8, 128.9, 118.4, 32.1, 29.6, 29.5 (2C), 27.2, 25.9, 22.9, 14.4. MS (ESI+) *m*/*z* (%): 310.2014 (100) $[M + H]^+$, 332.1830 (72) $[M + Na]^+$, 641.3785 (20) $[2M + Na]^+$.

*4-(1-(Quinolin-2-yl)-1H-1,2,3-triazol-4-yl)butan-1-ol (**4**).* This compound was obtained following the general procedure A at 125 °C for 30 h starting from tetrazolo[1,5-*a*]quinoline (**2**; 100.0 mg, 0.59 mmol, 1.0 equiv) and hexyn-1-ol (72.1 μL, 0.65 mmol, 1.1 equiv) after column chromatography on silica gel (eluent DCM/MeOH 96/4) as a pale yellow solid (122.6 mg, 78% chemical yield).

R_f (DCM/MeOH 94/6) = 0.175. ^{1}H NMR (300 MHz, $CDCl_3$): δ (ppm) 8.59 (s, 1H), 8. 35 (s, 2H), 8.04 (d, *J* = 8.7 Hz, 1H), 7.89 (d, *J* = 8.1 Hz, 1H), 7.78 (t, *J* = 8.7 Hz, 1H), 7.59 (t, *J* = 8.7 Hz, 1H), 3.73 (t, *J* = 6.3 Hz, 2H), 2.91 (t, *J* = 7.5 Hz, 2H), 2.0 (br s, 1H), 1.90 (quint, *J* = 7.2 Hz, 2H), 1.72 (quint, *J* = 6.3 Hz, 2H). ^{13}C NMR (75 MHz, $CDCl_3$): δ (ppm) 148.0, 146.4 (2C), 139.5, 130.7, 128.8, 127.8, 127.76, 127.0, 112.6, 62.3, 32.2, 25.5, 25.4. MS (ESI+) *m*/*z* (%): 291.1208 (100) $[M + Na]^+$.

Hex-5-ynoic Acid. Hex-5-yn-1-ol (1.00 g, 10.2 mmol, 1.0 equiv) was dissolved in acetone (80 mL) and cooled to 0 °C. Fresh Jones reagent was added dropwise to the solution with vigorous stirring until the reacting mixture remained orange. The mixture was warmed to room temperature, and more Jones reagent was added to maintain the orange color. One hour after the end of the addition, isopropyl alcohol (15 mL) was added; the mixture was filtered through Celite, and the solvent was evaporated under reduced pressure. The crude blue oil was dissolved in Et_2O (100 mL) and washed with water (3 × 75 mL). The organic phase was dried over $MgSO_4$, filtered, and evaporated to afford hex-5-ynoic acid as a yellow oil (761.0 mg, 67% chemical yield). The analytical data were in accordance with those in the literature.[12]

dx.doi.org/10.1021/ic5007007 | *Inorg. Chem.* 2014, 53, 6204−6223

^{1}H NMR (300 MHz, $CDCl_3$): δ (ppm) 11.18 (s, 1H), 2.43 (t, J = 7.4 Hz, 2H), 2.20 (t, J = 6.9 Hz, 2H), 1.96 (s, 1H), 1.76 (quint, J = 6.8 Hz, 2H).

Methyl Hex-5-ynoate. Hex-5-ynoic acid (761.0 mg, 6.79 mmol, 1.0 equiv) was dissolved in MeOH (2.5 mL) and DCM (8 mL). Three drops of 95% H_2SO_4 were added, and the solution was stirred under reflux for 24 h. The mixture was diluted with DCM (20 mL), and a saturated aqueous $NaHCO_3$ solution (20 mL) was added. The aqueous layer was further extracted with DCM (20 mL). The combined organic layers were dried over $MgSO_4$, filtered, and evaporated. The residue was purified by column chromatography on silica gel (DCM) to afford methyl hex-5-ynoate as a colorless oil (712.0 mg, 83% chemical yield). The analytical data were in accordance with those in the literature.[13]

R_f (DCM) = 0.85. ^{1}H NMR (300 MHz, $CDCl_3$): δ (ppm) 3.59 (s, 3H), 2.37 (t, J = 7.4 Hz, 2H), 2.18 (t, J = 7.4 Hz, 2H), 1.93 (s, 1H), 1.76 (quint, J = 7.1 Hz, 2H).

*Methyl 4-(1-(Quinolin-2-yl)-1H-1,2,3-triazol-4-yl)butanoate (**5**).* This compound was obtained following the general procedure A at 110 °C for 3 days starting from tetrazolo[1,5-*a*]quinoline (**2**; 100.0 mg, 0.59 mmol, 1.0 equiv) and methyl hex-5-ynoate (82.0 mg, 0.65 mmol, 1.12 equiv) after column chromatography on silica gel (eluent DCM/MeOH 99/1) as a yellow oil (118.0 mg, 67% chemical yield).

R_f (99/1 DCM/methanol) = 0.53. ^{1}H NMR (300 MHz, $CDCl_3$): δ (ppm) 8.49 (s, 1H), 8.24 (s, 2H), 7.94 (d, J = 8.4 Hz, 1H), 7.78 (d, J = 8.0 Hz, 1H), 7.68 (t, J = 7.7 Hz, 1H), 7.48 (t, J = 7.5 Hz, 1H), 3.61 (s, 3H), 2.82 (t, J = 7.5 Hz, 2H), 2.38 (t, J = 7.4 Hz, 2H), 2.05 (quint, J = 7.4 Hz, 2H). ^{13}C NMR (75 MHz, $CDCl_3$): δ (ppm) 173.7, 148.0, 147.9, 146.5, 139.6, 130.8, 128.9, 127.9, 127.8, 127.0, 118.6, 112.6, 51.7, 33.4, 25.0, 24.5.

*4-(1-(Quinolin-2-yl)-1H-1,2,3-triazol-4-yl)butanoic Acid (**6**).* Methyl 4-(1-(quinolin-2-yl)-1*H*-1,2,3-triazol-4-yl)butanoate (**5**; 63.0 mg, 0.213 mmol, 1.0 equiv) was dissolved in acetone. An aqueous NaOH solution was added (680 μL, 0.85 mmol, 4.0 equiv., 5% m/v), and the solution was stirred at 50 °C under Ar for 16 h. DCM and H_2O were added; the organic phase was discarded and the aqueous phase was acidified to pH 1 by addition of concentrated HCl. The resulting precipitate was extracted twice with a DCM/MeOH 9/1 mixture, and the organic phase was dried over Na_2SO_4, filtered, and evaporated to afford 4-(1-(quinolin-2-yl)-1*H*-1,2,3-triazol-4-yl)butanoic acid (**6**) as a white solid (60.0 mg, quantitative chemical yield).

^{1}H NMR (300 MHz, DMSO-d_6): δ (ppm) 12.14 (br s, 1H), 8.79 (s, 1H), 8.68 (d, J = 8.7 Hz, 1H), 8.28 (d, J = 8.7 Hz, 1H), 8.11 (d, J = 7.2 Hz, 1H), 8.04 (d, J = 8.4 Hz, 1H), 7.87 (t, J = 7.2 Hz, 1H), 7.68 (t, J = 8.4 Hz, 1H), 2.80 (t, J = 7.5 Hz, 2H), 2.33 (t, J = 7.2 Hz, 2H), 1.94 (quint, J = 7.2 Hz, 2H). ^{13}C NMR (75 MHz, DMSO-d_6): δ (ppm) 174.1, 147.7, 147.5, 145.7, 140.4, 131.1, 128.2, 127.5, 127.1, 119.1, 112.4, 33.0, 24.3, 24.1. MS (ESI+) m/z (%): 305.0998 (100) $[M + Na]^+$.

*2-(4-Octyl-1H-1,2,3-triazol-1-yl)quinoline (**7**).* This compound was obtained following the general procedure A starting from tetrazolo[1,5-*a*]quinoline (**2**; 100.0 mg, 0.59 mmol, 1.0 equiv) and 1-decyne (116 μL, 0.645 mmol, 1.1 equiv) after column chromatography on silica gel (eluent cyclohexane/EtOAc 80/20) as a pale yellow solid (117.0 mg, 56% chemical yield).

R_f (cyclohexane/EtOAc 80/20) = 0.29. ^{1}H NMR (300 MHz, $CDCl_3$): δ (ppm) 8.49 (s, 1H), 8.29 (t, 2H), 7.99 (d, J = 8.4 Hz, 1H), 7.82 (d, J = 8.1 Hz, 1H), 7.72 (t, J = 7.6 Hz, 1H), 7.52 (t, J = 7.5 Hz, 1H), 2.81 (t, J = 7.7 Hz, 2H), 1.75 (quint, J = 7.5 Hz, 2H), 1.58−1.07 (m, 10H), 1.00−0.66 (m, 3H). ^{13}C NMR (75 MHz, $CDCl_3$): δ (ppm) 146.5, 139.5, 130.7, 128.8, 127.84, 127.8, 126.9, 118.3, 112.7, 100.0, 31.9, 29.4, 29.32, 29.28, 29.25, 25.7, 22.7, 14.1. MS (ESI+) m/z (%): 309.2057 (100) $[M + H]^+$, 331.1877 (74) $[M + Na]^+$.

*2-(4-Dodecyl-1H-1,2,3-triazol-1-yl)quinoline (**8**).* This compound was obtained following the general procedure A at 120 °C for 24 h starting from tetrazolo[1,5-*a*]quinoline (**2**; 200.0 mg, 1.18 mmol, 1.0 equiv) and 1-tetradecyne (318 μL, 1.29 mmol, 1.1 equiv) after column chromatography on silica gel (eluent cyclohexane/EtOAc 80/20) as a pale yellow solid (323.0 mg, 75% chemical yield).

R_f (eluent cyclohexane/EtOAc 80/20) = 0.30. ^{1}H NMR (300 MHz, $CDCl_3$): δ (ppm) 8.50 (s, 1H), 8.30 (t, 2H), 8.01 (d, J = 8.5 Hz, 1H), 7.83 (d, J = 8.1 Hz, 1H), 7.77−7.69 (m, 1H), 7.54 (t, J = 7.5 Hz, 1H), 2.82 (t, J = 7.7 Hz, 2H), 1.76 (quint, J = 7.6 Hz, 2H), 1.48−1.24 (m, 18H), 0.86 (t, J = 6.6 Hz, 3H); ^{13}C NMR (75 MHz, $CDCl_3$): δ (ppm) 149.1, 148.1, 146.4, 139.4, 130.6, 128.8, 127.8, 126.8, 118.2, 112.6, 31.9, 29.70, 29.68, 29.67, 29.59, 29.44, 29.38, 29.32, 29.29, 26.9, 25.8, 22.7, 14.2. MS (ESI+) m/z (%): 365.2684 (100) $[M + H]^+$, 387.2502 (34) $[M + Na]^+$.

General Procedure B for Rhenium Coordination. The ligand (1.0 equiv) was suspended in anhydrous toluene (1.0 mL for 70.0 μmol) and heated at 110 °C under N_2 until complete dissolution. Bromopentacarbonylrhenium(I) (1.0 equiv) was added, the color of the solution changed, and gas was released. The solution was stirred at 110 °C under N_2 for 6 h. The mixture was cooled to room temperature and evaporated. The residue was purified by column chromatography on silica gel to afford the desired bromotricarbonylrhenium complex.

*[2-(4-Octyl-1H-1,2,3-triazol-1-yl)quinoxaline]-bromotricarbonylrhenium (**A**).* This compound was obtained according to general procedure B starting from 2-(4-octyl-1*H*-1,2,3-triazol-1-yl)quinoxaline (**3**; 26.0 mg, 84.0 μmol, 1.0 equiv) after column chromatography on silica gel (cyclohexane/EtOAc 7/3 to 5/5) as a deep red solid (47.0 mg, 76% chemical yield).

R_f (cyclohexane/EtOAc 5/5) = 0.48. ^{1}H NMR (300 MHz, $CDCl_3$): δ (ppm) 9.36 (s, 1H), 8.35 (d, J = 8.7 Hz, 1H), 8.49 (s, 1H), 8.33 (d, J = 8.4 Hz, 1H), 8.16 (t, J = 7.5 Hz, 1H), 8.05 (t, J = 7.5 Hz, 1H), 2.92 (td_{app}, J = 3.0, 7.5 Hz, 2H), 1.82 (quint, J = 7.5 Hz, 2H), 1.47−1.25 (m, 10H), 0.90 (m, 3H). ^{13}C NMR (75 MHz, $CDCl_3$): δ (ppm) 196.3, 193.1, 186.8, 154.1, 143.6, 142.1, 139.7, 135.5, 135.0, 133.2, 131.4, 130.4, 120.8, 32.4, 29.8, 29.7 (2C), 29.1, 26.3, 23.2, 14.7. HRMS (ESI+): calcd for $C_{21}H_{23}BrN_5NaO_3Re$ 682.0439, found 682.0413. HPLC (0 to 100% ACN in 30 min, column C8A): rt 26.97 (95%). IR: ν_{max}/cm^{-1} 2033, 1953, 1934, 1915 (CO).

*[4-(1-(Quinolin-2-yl)-1H-1,2,3-triazol-4-yl)butan-1-ol]-bromotricarbonylrhenium(I) (**B**).* This compound was obtained according to general procedure B starting from 4-(1-(quinolin-2-yl)-1*H*-1,2,3-triazol-4-yl)butan-1-ol (**4**; 75.0 mg, 0.28 mmol, 1.0 equiv) after filtering, washing with toluene, and drying under vacuum as a bright yellow solid (145.0 mg, 84% chemical yield). ^{1}H NMR (300 MHz, MeOD): δ (ppm) 9.23 (s, 1H), 8.89 (d, J = 8.7 Hz, 1H), 7.74 (d, J = 8.7 Hz, 1H), 8.34 (d, J = 8.7 Hz, 1H), 8.20 (dd, J = 1.2, 8.4 Hz, 1H), 8.11 (ddd, J = 1.5, 7.2, 8.7 Hz, 1H), 7.87 (ddd, J = 0.9, 7.2, 8.1 Hz, 1H), 3.66 (t, J = 6.3 Hz, 2H), 2.97 (t, J = 7.5 Hz, 2H), 1.93 (quint, J = 7.5 Hz, 2H), 1.70 (quint, J = 6.3 Hz, 2H). ^{13}C NMR (75 MHz, DMSO-d_6): δ (ppm) 153.5, 149.7, 146.7, 145.1, 134.4, 130.7, 130.4, 129.9, 129.4, 124.1, 112.7, 62.2, 32.6, 25.9 (2C). MS (ESI+) m/z (%): 640.9784 (48) $[M + Na]^+$, 539.0721 (100) $[M - Br]^+$, 291.1216 (56) $[M - Re(CO)_3Br + Na]^+$. HRMS (ESI+): calcd for $C_{18}H_{16}BrN_4NaO_4Re$ 640.9810, found 640.9784. HPLC (0 to 100% ACN in 30 min, column C8A): rt 19.85 (99.2%). IR: ν_{max}/cm^{-1} 2027, 1923, 1903 (CO).

*[4-(1-(Quinolin-2-yl)-1H-1,2,3-triazol-4-yl)butanoic acid]-bromotricarbonylrhenium(I) (**C**).* This compound was obtained according to general procedure B starting from 4-(1-(quinolin-2-yl)-1*H*-1,2,3-triazol-4-yl)butanoic acid (**6**; 53.0 mg, 0.19 mmol, 1.0 equiv) after filtering, washing with toluene, and drying under vacuum as a bright yellow solid (90.0 mg, 76% chemical yield).

^{1}H NMR (300 MHz, DMSO-d_6): δ (ppm) 12.19 (br s, 1H), 9.69 (s, 1H), 9.14 (d, J = 9.0 Hz, 1H), 8.62 (d, J = 8.7 Hz, 1H), 8.58 (d, J = 9.0 Hz, 1H), 8.32 (d, J = 8.4 Hz, 1H), 8.22 (td, J = 1.5, 7.5 Hz, 1H), 7.94 (t, J = 7.5 Hz, 1H), 2.92 (t, J = 7.5 Hz, 2H), 2.41 (t, J = 7.5 Hz, 2H), 1.99 (quint, J = 7.5 Hz, 2H). ^{13}C NMR (75 MHz, CD_3OD): δ (ppm) 183.7, 157.3, 157.1, 155.3, 150.0, 140.7, 137.8, 137.7, 137.0, 136.7, 128.7, 122.0, 42.5, 33.8, 33.6. MS (ESI+) m/z (%): 654.9583 (88) $[M + Na]^+$, 553.0514 (100) $[M - Br]^+$, 305.1014 (88) $[M - Re(CO)_3Br + Na]^+$. HRMS (ESI+): calcd for $C_{18}H_{14}BrN_4NaO_5Re$ 654.9580, found 640.9583. HPLC (40 to 100% ACN in 30 min, column C18-300): rt 9.64 min (95.5%). IR: ν_{max}/cm^{-1} 2024, 1936, 1884 (CO).

*[2-(4-Octyl-1H-1,2,3-triazol-1-yl)quinoline]-bromotricarbonylrhenium(I) (**D**).* This compound was obtained according to general procedure B starting from 2-(4-octyl-1*H*-1,2,3-triazol-1-yl)quinoline (**7**; 60.0 mg, 195 μmol, 1.0 equiv) after

dx.doi.org/10.1021/ic5007007 | *Inorg. Chem.* 2014, 53, 6204−6223

purification by column chromatography on silica gel (cyclohexane/EtOAc 50/50) as a yellow solid (85 mg, 66% chemical yield).

R_f (cyclohexane/EtOAc 50/50) = 0.34. ^{1}H NMR (300 MHz, $CDCl_3$): δ (ppm) 8.75 (d, J = 8.8 Hz, 1H), 8.49 (t, J = 4.4 Hz, 2H), 8.01 (m, 1H), 7.97−7.86 (m, 2H), 7.74 (t, J = 7.3 Hz, 1H), 2.85−2.62 (m, 2H), 1.69 (tt, J = 12.9, 6.7 Hz, 2H), 1.30 (m, 10H), 0.94−0.82 (m, 3H). ^{13}C NMR (75 MHz, $CDCl_3$): δ (ppm) 196.7, 193.6, 187.3, 153.0, 147.7, 146.0, 143.7, 134.2, 130.4, 129.4, 129.2, 127.9, 121.3, 111.0, 31.8, 29.21, 29.18, 29.17, 26.9, 25.6, 22.7, 14.2. MS (ESI+) m/z (%): 681.0450 (100) $[M + Na]^+$, 579.1380 (100) $[M - Br]^+$. HRMS (ESI+): calcd for $C_{22}H_{24}BrN_4NaO_3Re$ 681.0464, found 681.0450. HPLC (40 to 100% ACN in 30 min, column C18-300): rt 23.07 (96.6%). IR: ν_{max}/cm^{-1} 2024, 1923, 1901 (CO).

*[2-(4-Dodecyl-1H-1,2,3-triazol-1-yl)quinoline]-bromotricarbonylrhenium(I) (**E**).* This compound was obtained according to general procedure B starting from 2-(4-dodecyl-1*H*-1,2,3-triazol-1-yl)quinoline (**8**; 60.0 mg, 165 μmol, 1.0 equiv) after purification by column chromatography on silica gel (cyclohexane/EtOAc 50/50) as a yellow solid (86.0 mg, 72% chemical yield).

R_f (cyclohexane/EtOAc 50/50) = 0.36. ^{1}H NMR (300 MHz, $CDCl_3$): δ (ppm) 8.77 (d, J = 8.8 Hz, 1H), 8.48 (d, J = 8.7 Hz, 2H), 8.02 (t, J = 7.6 Hz, 1H), 7.91 (dd, J = 12.4, 8.6 Hz, 2H), 7.75 (t, J = 7.4 Hz, 1H), 2.86−2.63 (m, J = 7.8 Hz, 2H), 1.78−1.58 (m, 2H), 1.48−1.18 (m, 18H), 0.87 (t, J = 6.6 Hz, 3H). ^{13}C NMR (75 MHz, $CDCl_3$): δ (ppm) 195.6, 192.4, 186.3, 170.2, 151.9, 146.7, 145.0, 142.5, 133.1, 129.4, 128.3, 128.1, 126.8, 120.1, 109.8, 59.4, 30.9, 28.7, 28.2, 27.6, 25.9, 24.6, 21.7, 20.0, 13.2, 13.1. MS (ESI+) m/z (%): 737.1066 (100) $[M + Na]^+$. HRMS (ESI+): calcd for $C_{26}H_{32}BrN_4NaO_3Re$ 737.1091, found 737.1066. HPLC (40 to 100% ACN in 30 min, column C18-300): rt 29.46 (98.1%). IR: ν_{max}/cm^{-1} 2032, 1933, 1904, 1850 (CO).

6-Azidohexan-1-ol. 6-Bromohexan-1-ol (1.0 g, 5.52 mmol, 1.0 equiv) was dissolved in an acetone/H_2O 3/1 mixture (20 mL), and NaN_3 (719.0 mg, 11.05 mmol, 2.0 equiv) was added. The solution was stirred at room temperature under Ar overnight. The mixture was diluted with H_2O and extracted twice with DCM. The organic phase was washed with saturated brine, dried over $MgSO_4$, filtered, and evaporated to afford 6-azidohexan-1-ol as a yellow oil (697.0 mg, 88% chemical yield). The analytical data were in accordance with those in the literature.[14a]

^{1}H NMR (300 MHz, $CDCl_3$): δ (ppm) 3.65 (t, J = 0.6 Hz, 2H), 3.27 (t, J = 0.6 Hz, 2H), 1.60 (m, 4H), 1.40 (m, 4H).

*6-(4-(Quinolin-2-yl)-1,2,3-triazol-1-yl)hexanol (**11**).* 2-Ethynylquinoline[9] (**10**; 50.0 mg, 0.33 mmol, 1.0 equiv) was suspended in *tert*-butyl alcohol (4.4 mL). 6-Azidohexanol (51.5 mg, 0.36 mmol, 1.1 equiv), an aqueous solution of $CuSO_4{\cdot}5H_2O$ (2.056 mL, 32.6 μmol, 0.1 equiv, from a 4.12 mg mL^{-1} solution in water), and an aqueous solution of sodium ascorbate (2.317 mL, 0.098 mmol, 0.3 equiv, from a 8.7 mg mL^{-1} solution in water) were then added. The resulting mixture was stirred at 110 °C under Ar for 4 h. The mixture was diluted with H_2O and extracted twice with DCM. The organic phase was dried over $MgSO_4$, filtered, and evaporated. The residue was purified by column chromatography on silica gel (eluent DCM/MeOH 95/5) to afford 6-(4-(quinolin-2-yl)-1,2,3-triazol-1-yl)-hexanol (**11**) as a pale yellow solid (47.7 mg, 49% chemical yield).

^{1}H NMR (300 MHz, $CDCl_3$): δ (ppm) 8.44 (s, 1H), 8.35 (d, J = 8.7 Hz, 1H), 8.25 (d, J = 8.7 Hz, 1H), 8.09 (d, J = 8.4 Hz, 1H), 7.82 (d, J = 7.8 Hz, 1H), 7.72 (ddd, J = 1.2, 6.9, 8.4 Hz, 1H), 7.52 (t, J = 7.8 Hz, 1H), 4.45 (t, J = 6.9 Hz, 2H), 3.62 (t, J = 6.0 Hz, 2H), 1.98 (quint, J = 6.9 Hz, 2H), 1.56 (quint, J = 6.6 Hz, 2H), 1.48−1.34 (m, 4H). ^{13}C NMR (75 MHz, $CDCl_3$): δ (ppm) 150.5, 148.3, 147.7, 137.4, 130.1, 128.7, 127.92, 127.0, 126.6, 123.1, 118.8, 62.4, 50.5, 32.4, 30.2, 26.1, 25.1. HRMS (ESI+): calcd for $C_{17}H_{20}N_4NaO$ 319.15293, found 319.15288.

*2-(1-Dodecyl-1,2,3-triazol-4-yl)quinoline (**12**).* 2-Ethynylquinoline[9] (**10**; 34.0 mg, 0.22 mmol, 1.0 equiv) was suspended in *tert*-butyl alcohol (3.0 mL). 1-Dodecyl azide (51.5 mg, 0.24 mmol, 1.1 equiv), an aqueous solution of $CuSO_4{\cdot}5H_2O$ (1.40 mL, 22.2 μmol, 0.1 equiv., from a 4.12 mg mL^{-1} solution in water), and an aqueous solution of sodium ascorbate (1.575 mL, 0.067 mmol, 0.3 equiv, from a 8.7 mg mL^{-1} solution in water) were then added. The resulting mixture was stirred at 110 °C under Ar for 4 h. The mixture was diluted with H_2O and extracted twice with DCM. The organic phase was dried over $MgSO_4$, filtered, and evaporated. The residue was purified by column chromatography on silica gel (eluent cyclohexane/EtOAc 5/5) to afford 2-(1-dodecyl-4−1,2,3-triazolyl)quinoline (**12**) as a pale yellow solid (15.3 mg, 19% chemical yield).

^{1}H NMR (300 MHz, $CDCl_3$): δ (ppm) 8.34 (m, 2H), 8.23 (d, J = 8.7 Hz, 1H), 8.05 (d, J = 8.7 Hz, 1H), 7.81 (d, J = 8.1 Hz, 1H), 7.70 (ddd, J = 1.5, 6.9, 8.4 Hz, 1H), 7.51 (ddd, J = 1.2, 6.9, 8.1 Hz, 1H), 4.43 (t, J = 7.2 Hz, 2H), 1.97 (quint, J = 7.2 Hz, 2H), 1.35−1.26 (m, 18H), 0.86 (t, J = 6.9 Hz, 3H).

*[6-(4-(Quinolin-2-yl)-1,2,3-triazol-1-yl)hexanol]-bromotricarbonylrhenium(I) (**F**).* This compound was obtained according to general procedure B starting from 6-(4-(quinolin-2-yl)-1,2,3-triazol-1-yl)hexanol (**11**; 25.0 mg, 84.4 μmol, 1.0 equiv) after purification by column chromatography on silica gel (DCM/MeOH 96/4) as a yellow solid (31.8 mg, 58% chemical yield).

^{1}H NMR (300 MHz, d_6-acetone): δ (ppm) 9.29 (s, 1H), 8.35 (d, J = 9.0 Hz, 1H), 8.35 (d, J = 8.7 Hz, 1H), 8.31 (d, J = 8.7 Hz, 1H), 8.19 (dd, J = 1.5, 8.4 Hz, 1H), 8.11 (ddd, J = 1.5, 7.2, 8.7 Hz, 1H), 7.85 (ddd, J = 1.2, 7.2, 8.1 Hz, 1H), 4.77 (t, J = 7.2 Hz, 2H), 3.53 (t, J = 6.0 Hz, 2H), 3.45 (t, J = 5.7 Hz, 1H, OH), 2.12 (q, J = 6.9 Hz, 2H), 1.55−1.48 (m, 6H). ^{13}C NMR (75 MHz, d_6-acetone): δ (ppm) 199.0 (CO), 196.5 (CO), 189.7 (CO), 152.9, 151.2, 148.1, 142.1, 133.4, 130.9, 130.2, 129.5, 129.3, 127.4, 120.1, 62.2, 53.0, 33.4, 30.5, 26.7, 26.0; MS (ESI+) m/z (%): 669.0069 (100) $[M + Na]^+$, 567.1010 (19) $[M - Br]^+$. HRMS (ESI+): calcd for $C_{20}H_{20}BrN_4NaO_4Re$ 669.0123, found 669.0069. HPLC (40 to 100% ACN in 20 min, column C18): rt 10.20 (96.5%). IR: ν_{max}/cm^{-1} 2020, 1892 (CO).

*[2-(1-Dodecyl-1,2,3-triazol-4-yl)quinoline]-bromotricarbonylrhenium(I) (**G**).* This compound was obtained according to general procedure B starting from 2-(1-dodecyl-1,2,3-triazol-4-yl)quinoline (**12**; 10.0 mg, 27.4 μmol, 1.0 equiv) after purification by column chromatography on silica gel (DCM) as a yellow solid (14.9 mg, 76% chemical yield).

^{1}H NMR (300 MHz, d_6-acetone): δ (ppm) 9.27 (s, 1H), 8.85−8.80 (m, 2H), 8.31 (d, J = 8.4 Hz, 1H), 8.19 (dd, J = 1.5, 8.1 Hz, 1H), 8.12 (ddd, J = 1.5, 6.9, 8.7 Hz, 1H), 7.86 (ddd, J = 1.2, 6.9, 8.4 Hz, 1H), 4.77 (t, J = 6.9 Hz, 2H), 2.11 (q, J = 6.9 Hz, 2H), 1.46−1.42 (m, 4H), 1.30−1.26 (m, 14H), 0.86 (t, J = 6.9 Hz, 3H). ^{13}C NMR (75 MHz, d_6-acetone): δ (ppm) 152.9, 151.3, 148.2, 142.2, 133.5, 131.0, 130.3, 129.6, 129.4, 127.5, 120.2, 53.1, 32.7, 30.6, 30.3, 30.1, 27.0, 23.4, 14.4. MS (ESI+) m/z (%): 737.1078 (100) $[M + Na]^+$. HRMS (ESI+): calcd for $C_{26}H_{32}BrN_4NaO_3Re$ 737.1091, found 737.1066. HPLC (40 to 100% ACN in 20 min, column C18): rt 22.65 (100.0%). IR: ν_{max}/cm^{-1} 2022, 1921, 1895, 1854 (CO).

*Tetrazolo[1,5-a]pyridine (**13**).* Pyridine (808 μL, 10.0 mmol, 1.6 equiv) was added to a mixture of pyridine *N*-oxide (600.0 mg, 6.3 mmol, 1.0 equiv) and diphenylphosphoryl azide (DPPA; 2.154 mL, 10.0 mmol, 1.6 equiv), and the mixture was stirred at 120 °C under Ar for 24 h. The mixture was evaporated to dryness and the residue purified by column chromatography on silica gel (DCM/MeOH 99/1) to afford tetrazolo[1,5-*a*]pyridine (**13**) as a white fluffy solid (718.0 mg, 95%). The analytical data were in accordance with those in the literature.[8]

R_f (DCM/methanol 99.5/0.5) = 0.84. ^{1}H NMR (300 MHz, $CDCl_3$): δ (ppm) 8.84 (dt, J = 1.0, 6.9 Hz, 1H), 8.03 (dt, J = 1.0, 9.0 Hz, 1H), 7.68 (ddd, J = 1.0, 6.9, 9.0 Hz, 1H), 7.25 (td, J = 0.9, 6.9 Hz, 1H). ^{13}C NMR (75 MHz, $CDCl_3$): δ (ppm) 148.6, 132.1, 125.5, 116.8, 116.0.

*4-(1-(Pyridin-2-yl)-1H-1,2,3-triazol-4-yl)butan-1-ol (**14**).* This compound was obtained following the general procedure A at 100 °C for 8 h starting from tetrazolo[1,5-*a*]pyridine (**13**; 75.0 mg, 0.62 mmol, 1.0 equiv) and hexyn-1-ol (76.6 μL, 0.69 mmol, 1.1 equiv) after column chromatography on silica gel (eluent DCM/MeOH 94/6) as a yellow oil (108.0 mg, 79% chemical yield).

^{1}H NMR (300 MHz, $CDCl_3$): δ (ppm) 8.33 (ddd, J = 0.6, 1.8, 4.8 Hz, 1H), 8.22 (s, 1H), 8.01 (d, J = 8.4 Hz, 1H), 7.77 (ddd, J = 1.8, 7.5, 8.1 Hz, 1H), 7.19 (ddd, J = 0.9, 4.8, 7.5 Hz, 1H), 3.60 (t, J = 6.3 Hz, 2H), 2.72 (t, J = 7.5 Hz, 2H), 1.73 (quint, J = 7.5 Hz, 2H), 1.56 (quint, J = 6.3 Hz, 2H). ^{13}C NMR (75 MHz, $CDCl_3$): δ (ppm) 149.1, 148.5,

dx.doi.org/10.1021/ic5007007 | Inorg. Chem. 2014, 53, 6204−6223

148.4, 139.1, 123.4, 118.3, 113.6, 61.9, 32.1, 25.5, 25.3. MS (ESI+) *m*/*z* (%): 241.1055 (100) $[M + Na]^+$.

*2-(4-Butyl-1H-1,2,3-triazol-1-yl)pyridine (**15**).* This compound was obtained following the general procedure A at 110 °C for 48 h starting from tetrazolo[1,5-*a*]pyridine (**13**; 70.0 mg, 0.58 mmol, 1.0 equiv) and 1-hexyne (73.7 μL, 0.64 mmol, 1.1 equiv) after column chromatography on silica gel (cyclohexane/EtOAc 70/30) as a brown oil (77.0 mg, 65% chemical yield).

R_f (cyclohexane/EtOAc 70/30) = 0.76. ^{1}H NMR (300 MHz, $CDCl_3$): δ (ppm) 8.42 (m, 1H), 8.27 (s, 1H), 8.12 (m, 1H), 7.84 (m, 1H), 7.26 (m, 1H), 2.76 (t, *J* = 7.5 Hz, 2H), 1.67 (quint, *J* = 7.5 Hz, 2H), 1.36 (sext, *J* = 7.5 Hz, 2H), 0.89 (t, *J* = 7.5 Hz, 3H). ^{13}C NMR (75 MHz, $CDCl_3$): δ (ppm) 149.3, 149.2, 148.4, 139.0, 123.3, 118.2, 113.7, 31.4, 25.4, 22.2, 13.8. MS (ESI+) *m*/*z* (%): 203.1286 (100) $[M + H]^+$, 225.1108 (64) $[M + Na]^+$.

*2-(4-Octyl-1H-1,2,3-triazol-1-yl)pyridine (**16**).* This compound was obtained following the general procedure A at 120 °C for 24 h starting from tetrazolo[1,5-*a*]pyridine (**13**; 100.0 mg, 0.833 mmol, 1.0 equiv) and 1-decyne (166 μL, 0.92 mmol, 1.1 equiv) after column chromatography on silica gel (cyclohexane/EtOAc 80/20) as a pale yellow solid (135.0 mg, 62% chemical yield).

R_f (cyclohexane/EtOAc 80/20) = 0.13. ^{1}H NMR (300 MHz, $CDCl_3$): δ (ppm) 8.46 (d, *J* = 4.9, 1.7 Hz, 1H), 8.29 (s, 1H), 8.16 (d, *J* = 8.2 Hz, 1H), 7.87 (td, *J* = 7.8, 1.8 Hz, 1H), 7.34−7.27 (m, 1H), 2.78 (t, *J* = 7.6 Hz, 2H), 1.71 (q, *J* = 7.8 Hz, 2H), 1.46−1.21 (m, 10 H), 0.95−0.82 (m, 3H). ^{13}C NMR (75 MHz, $CDCl_3$): δ (ppm) 149.4, 149.0, 148.4, 139.0, 123.2, 118.1, 113.7, 31.9, 29.4, 29.3, 29.2, 25.7, 22.7, 14.1. MS (ESI+) *m*/*z* (%): 259.1902 (100) $[M + H]^+$, 281.1722 (83) $[M + Na]^+$.

*2-(4-Dodecyl-1H-1,2,3-triazol-1-yl)pyridine (**17**).* This compound was obtained following the general procedure A at 120 °C for 24 h starting from tetrazolo[1,5-*a*]pyridine (**13**; 150.0 mg, 1.25 mmol, 1.0 equiv) and 1-tetradecyne (341 μL, 1.38 mmol, 1.1 equiv) after column chromatography on silica gel (cyclohexane/EtOAc 80/20) as a pale yellow solid (278.0 mg, 70% chemical yield).

R_f (cyclohexane/EtOAc 80/20) = 0.12. ^{1}H NMR (300 MHz, $CDCl_3$): δ (ppm) 8.37 (d, *J* = 4.1 Hz, 1H), 8.21 (s, 1H), 8.07 (d, *J* = 8.2 Hz, 1H), 7.78 (t, *J* = 8.6 Hz, 1H), 7.2 (dd, 1H), 2.70 (t, *J* = 7.6 Hz, 2H), 1.64 (p, *J* = 7.5 Hz, 2 H), 1.24 (d, *J* = 48.3 Hz, 18 H), 0.77 (t, *J* = 6.5 Hz, 3H). ^{13}C NMR (75 MHz, $CDCl_3$): δ (ppm) 149.3, 148.8, 148.4, 138.9, 123.1, 118.0, 113.6, 31.9, 29.7, 29.6, 29.5, 29.4, 29.33, 29.25, 29.19, 26.9, 25.6, 22.7, 14.1. MS (ESI+) *m*/*z* (%): 315.2529 (100) $[M + H]^+$, 337.2349 (69) $[M + Na]^+$.

*[4-(1-(Pyridin-2-yl)-1H-1,2,3-triazol-4-yl)butan-1-ol]-bromotricarbonylrhenium(I) (**H**).* This compound was obtained according to general procedure B starting from 4-(1-(pyridin-2-yl)-1*H*-1,2,3-triazol-4-yl)butan-1-ol (**14**; 70.0 mg, 0.32 mmol, 1.0 equiv) after purification by column chromatography on silica gel (DCM/MeOH 92/8) as a bright yellow solid (138.0 mg, 86% chemical yield).

^{1}H NMR (300 MHz, MeOD): δ (ppm) 9.05 (s, 1H), 8.92 (d, *J* = 4.8 Hz, 1H), 8.34 (t_{app}, *J* = 4.8 Hz, 1H), 8.26 (d, *J* = 5.1 Hz, 1H), 7.66 (t, *J* = 6.6 Hz, 1H), 3.62 (t, *J* = 6.3 Hz, 2H), 2.90 (t, *J* = 7.5 Hz, 2H), 1.86 (quint, *J* = 7.5 Hz, 2H), 1.66 (quint, *J* = 6.3 Hz, 2H). ^{13}C NMR (75 MHz, MeOD): δ (ppm) 153.6, 153.1, 148.8, 143.6, 127.0, 123.2, 115.2, 62.2, 32.6, 25.94, 25.91. MS (ESI+) *m*/*z* (%): 590.9636 (96) $[M + Na]^+$, 489.0569 (100) $[M - Br]^+$, 241.1063 (68) $[M - Re(CO)_3Br + Na]^+$. HRMS (ESI+): calcd for $C_{14}H_{14}BrN_4NaO_4Re$ 590.9631, found 590.9636. HPLC (0 to 100% ACN in 30 min, column C8A): rt 17.57 (90.8%). IR: ν_{max}/cm^{-1} 2022, 1934, 1884 (CO).

*[2-(4-Butyl-1H-1,2,3-triazol-1-yl)pyridine]-bromotricarbonylrhenium(I) (**I**).* This compound was obtained according to general procedure B starting from 2-(4-butyl-1*H*-1,2,3-triazol-1-yl)pyridine (**15**; 30.0 mg, 148 μmol, 1.0 equiv) after purification by column chromatography on silica gel (cyclohexane/EtOAc 30/70) as a yellow solid (59.5 mg, 73% chemical yield).

R_f (cyclohexane/EtOAc 30/70) = 0.24. ^{1}H NMR (300 MHz, $CDCl_3$): δ (ppm) 8.60 (dd, *J* = 1.2, 5.4 Hz, 1H), 8.24 (s, 1H), 8.18 (td_{app}, *J* = 1.2, 5.4 Hz, 1H), 7.83 (d, *J* = 8.1 Hz, 1H), 7.57−7.52 (m, 1H), 2.87−2.81 (m, 2H), 1.77−1.69 (m, 2H), 1.45 (sext, *J* = 7.5 Hz, 2H), 0.97 (t, *J* = 7.5 Hz, 3H). ^{13}C NMR (75 MHz, $CDCl_3$): δ (ppm) 153.3, 152.8, 147.5, 141.9, 125.8, 120.1, 113.4, 30.8, 25.5, 22.4, 13.9. MS (ESI+) *m*/*z* (%): 574.9681 (100) $[M + Na]^+$, 225.1108 (76) $[M - Re(CO)_3Br + Na]^+$. HRMS (ESI+): calcd for $C_{14}H_{14}BrN_4NaO_3Re$ 574.9682, found 574.9681. HPLC (40 to 100% ACN in 30 min, column C18A): rt 11.807 (87.6%), IR: ν_{max}/cm^{-1} 2025, 1896 (CO),

*[2-(4-Octyl-1H-1,2,3-triazol-1-yl)pyridine]-bromotricarbonylrhenium(I) (**J**).* This compound was obtained according to general procedure B starting from 2-(4-octyl-1*H*-1,2,3-triazol-1-yl)pyridine (**16**; 60.0 mg, 232 μmol, 1.0 equiv) after purification by column chromatography on silica gel (cyclohexane/EtOAc 50/50) as a yellow solid (123.0 mg, 87% chemical yield).

R_f (cyclohexane/EtOAc 50/50) = 0.28. ^{1}H NMR (300 MHz, $CDCl_3$): δ (ppm) 8.95−8.88 (dd, 1H), 8.34 (s, 1H), 8.18 (td, *J* = 8.3, 1.6 Hz, 1H), 7.91 (d, *J* = 8.3 Hz, 1H), 7.56−7.48 (m, 1H), 2.89−2.67 (m, 2H), 1.72 (p, *J* = 8.0, 7.5 Hz, 2H), 1.47−1.17 (m, 10H), 0.94−0.81 (m, 3H). ^{13}C NMR (75 MHz, $CDCl_3$): δ (ppm) 195.9, 194.0, 187.3, 152.9, 152.7, 147.4, 142.0, 125.7, 120.3, 113.5, 60.4, 31.8, 29.2, 28.6, 26.9, 25.7, 22.7, 14.1. MS (ESI+) *m*/*z* (%): 1137.1619 (32) $[2M - Br]^+$, 631.0297 (100) $[M + Na]^+$, 529.1231 (68) $[M - Br]^+$, 281.1739 (32) $[M - Re(CO)_3Br + Na]^+$. HRMS (ESI+): calcd for $C_{18}H_{22}BrN_4NaO_3Re$ 631.0308, found 631.0297. HPLC (40 to 100% ACN in 30 min, column C18-300): rt 20.47 (96.3%). IR: ν_{max}/cm^{-1} 2023, 1919, 1916, 1885 (CO).

*[2-(4-Dodecyl-1H-1,2,3-triazol-1-yl)pyridine]-bromotricarbonylrhenium(I) (**K**).* This compound was obtained according to general procedure B starting from 2-(4-dodecyl-1*H*-1,2,3-triazol-1-yl)pyridine (**17**; 100.0 mg, 318 μmol, 1.0 equiv) after purification by column chromatography on silica gel (cyclohexane/EtOAc 50/50) as a yellow solid (169.0 mg, 80% chemical yield).

R_f (cyclohexane/EtOAc 50/50) = 0.30. ^{1}H NMR (300 MHz, $CDCl_3$): δ (ppm) 8.95 (d, *J* = 5.3 Hz, 1H), 8.25 (s, 1H), 8.17 (t, *J* = 7.8 Hz, 1H), 7.84 (d, *J* = 8.2 Hz, 1H), 7.58−7.46 (m, 1H), 2.82 (h, *J* = 7.6 Hz, 2H), 1.73 (q, *J* = 7.7, 7.3 Hz, 2H), 1.26 (s, 18H), 0.88 (t, *J* = 6.4 Hz, 3H). ^{13}C NMR (75 MHz, $CDCl_3$): δ (ppm) 186.3, 152.0, 151.7, 146.4, 140.8, 124.6, 119.0, 112.3, 30.9, 28.64, 28.62, 28.61, 28.5, 28.3, 28.24, 28.19, 27.6, 24.7, 21.7, 13.1. MS (ESI+) *m*/*z* (%): 687.0920 (100) $[M + Na]^+$. HRMS (ESI+): calcd for $C_{22}H_{30}BrN_4NaO_3Re$ 687.0934, found 687.0920. HPLC (20 to 100% ACN in 20 min, column C18 A): 23.747 min (91.4%). IR: ν_{max}/cm^{-1} 2022, 1918, 1896, 1886 (CO).

*[2-(4-Dodecyl-1H-1,2,3-triazol-1-yl)pyridine]-chlorotricarbonylrhenium(I) (**L**).* This compound was obtained according to an adapted general procedure B starting from 2-(4-dodecyl-1*H*-1,2,3-triazol-1-yl)pyridine (**17**; 28.0 mg, 92.1 μmol, 1.0 equiv) and chloropentacarbonylrhenium(I) (35.0 mg, 96.7 μmol, 1.05 equiv) after purification by column chromatography on silica gel (cyclohexane/EtOAc 30/70) as a yellow solid (44.0 mg, 77% chemical yield).

^{1}H NMR (300 MHz, $CDCl_3$): δ (ppm) 8.89 (d, *J* = 5.4 Hz, 1H), 8.12 (m, 2H), 7.74 (d, *J* = 8.1 Hz, 1H), 7.47 (dd, *J* = 5.7, 7.2 Hz, 1H), 2.75 (m, 2H), 1.68 (quint, *J* = 7.2 Hz, 2H), 1.23 (m, 18H), 0.81 (t, *J* = 6.9 Hz, 3H). ^{13}C NMR (75 MHz, $CDCl_3$): δ (ppm) 153.2, 152.8, 147.7, 141.9, 125.8, 120.2, 113.4, 32.0, 29.79, 29.77, 29.76, 29.6, 29.5, 29.4, 29.36, 28.8, 25.8, 22.8, 14.3. MS (ESI+) *m*/*z* (%): 899.4322 (52) $[L_2Re(CO)_3]^+$, 643.1432 (100) $[M + Na]^+$, 585.1859 (48) $[M - Cl]^+$, 337.2349 (48) $[M - Re(CO)_3Cl + Na]^+$. HRMS (ESI+): calcd for $C_{22}H_{30}ClN_4NaO_3Re$ 643.1448, found 643.1432. HPLC (40 to 100% ACN in 30 min, column C18A): rt 21.754 (100%). IR: ν_{max}/cm^{-1} 2028, 1914 (CO).

*4-Bromobenzo[c][1,2,5]thiadiazole (**18**).* Benzothiadiazole (1.0 g, 7.34 mmol, 1.0 equiv) was suspended in HBr (33% in AcOH, 13 mL), and the mixture was stirred at 100 °C. Bromine (414 μL, 8.08 mmol, 1.1 equiv) was added slowly at 100 °C, and the solution was stirred at 115 °C for 2 h. Bromine (138 μL) was again added, and the mixture was stirred at 140 °C for 3.5 h. The mixture was diluted with H_2O; a saturated aqueous $Na_2S_2O_5$ solution was added until the discoloration was complete, and the solution was extracted with Et_2O and DCM. The combined organic phases were dried over $MgSO_4$, filtered, and evaporated. The residue was purified by column chromatoghaphy on silica gel (SiO_2, eluent cyclohexane/EtOAc 9/1). The fractions containing the desired compound were combined and evaporated.

dx.doi.org/10.1021/ic5007007 | *Inorg. Chem.* 2014, 53, 6204−6223

The residue was taken up in the minimum amount of EtOH. Successive recrystallizations afforded 4-bromobenzo[*c*][1,2,5]thiadiazole (**18**) as a white solid (352.0 mg, 22% chemical yield). The analytical data were in accordance with those in the literature.[15]

^{1}H NMR (300 MHz, $CDCl_3$): δ (ppm) 7.97 (dd, J = 0.9 Hz, 8.7 Hz, 1H), 7.84 (dd, J = 0.6 Hz, 7.2 Hz, 1H), 7.48 (dd, J = 7.5 Hz, 9.0 Hz, 1H).

*4-Ethynylbenzo[c][1,2,5]thiadiazole (**19**).* 4-Bromobenzo[*c*][1,2,5]thiadiazole (**18**; 150.0 mg, 0.70 mmol, 1.0 equiv) was dissolved in dry DMF (1.5 mL) and Et_3N (1.5 mL), and the solution was degassed and bubbled with Ar for 10 min. CuI (13.3 mg, 0.07 mmol, 0.1 equiv), $Pd(PPh_3)_4$ (40.3 mg, 0.035 mmol, 0.05 equiv), and (trimethylsilyl)acetylene (149 μL, 1.05 mmol, 1.5 equiv) were successively added, and the resulting pale orange mixture was stirred under Ar at 70 °C overnight. The mixture was evporated and the residue purified by column chromatography on silica gel (eluent DCM/petroleum ether 7/3) to afford 4-((trimethylsilyl)ethynyl)benzo[*c*][1,2,5]thiadiazole as a brownish yellow solid (55.0 mg, traces of starting material, used in the next step without further purification). The analytical data were in accordance with those in the literature.[16]

R_f (DCM/petroleum ether 7/3) = 0.59. ^{1}H NMR (300 MHz, $CDCl_3$): δ (ppm) 7.99 (dd, J = 1.2 Hz, 8.7 Hz, 1H), 7.77 (dd, J = 1.2 Hz, 7.2 Hz, 1H), 7.55 (dd, J = 7.2 Hz, 8.7 Hz, 1H), 0.34 (s, 9H).

4-((Trimethylsilyl)ethynyl)benzo[*c*][1,2,5]thiadiazole (61.0 mg, 0.26 mmol, 1.0 equiv) was dissolved in MeOH (4 mL). K_2CO_3 (36.3 mg, 0.26 mmol, 1.0 equiv) was added, and the solution was stirred at room temperature under Ar for 2 h. The mixture was diluted with H_2O and extracted twice with DCM. The organic phase was dried over $MgSO_4$, filtered, and evaporated. The residue was purified by column chromatography on silica gel (eluent cyclohexane/EtOAc 9/1) to afford 4-ethynylbenzo[*c*][1,2,5]thiadiazole (**19**) as a yellowish solid (25.0 mg, 34% chemical yield over two steps).

R_f (cyclohexane/EtOAc 9/1) = 0.30. ^{1}H NMR (300 MHz, $CDCl_3$): δ (ppm) 8.02 (dd, J = 0.9 Hz, 8.7 Hz, 1H), 7.78 (dd, J = 0.9 Hz, 6.9 Hz, 1H), 7.55 (dd, J = 6.9 Hz, 9.0 Hz, 1H), 3.59 (s, 1H). ^{13}C NMR (75 MHz, $CDCl_3$): δ (ppm) 154.8, 154.5, 133.8, 129.1, 122.7, 116.0, 83.7, 79.2.

*6-(4-(Benzo[c][1,2,5]thiadiazol-4-yl)-1H-1,2,3-triazol-1-yl)hexan-1-ol (**20**).* 4-Ethynylbenzo[*c*][1,2,5]thiadiazole (**19**; 20.0 mg, 0.12 mmol, 1.0 equiv) was suspended in *tert*-butyl alcohol (1.7 mL). 6-Azidohexanol (18.8 mg, 0.13 mmol, 1.05 equiv), an aqueous solution of $CuSO_4{\cdot}5H_2O$ (757.0 μL, 12.0 μmol, 0.1 equiv, from a 4.12 mg mL^{-1} solution in water), and an aqueous solution of sodium ascorbate (853.0 μL, 0.036 mmol, 0.3 equiv, from a 8.7 mg mL^{-1} solution in water) were then added. The resulting mixture was stirred at 110 °C under Ar overnight. The mixture was diluted with H_2O and extracted twice with DCM. The organic phase was dried over $MgSO_4$, filtered, and evaporated. The residue iswas purified by column chromatography on silica gel (eluent DCM/MeOH 94/6) to afford 6-(4-(benzo[*c*][1,2,5]thiadiazol-4-yl)-1*H*-1,2,3-triazol-1-yl)hexan-1-ol (**20**) as a yellow solid (34.0 mg, 90% chemical yield).

R_f (DCM/MeOH 94/6) = 0.26. ^{1}H NMR (300 MHz, $CDCl_3$): δ (ppm) 8.76 (s, 1H), 8.57 (dd, J = 0.9 Hz, 6.9 Hz, 1H), 7.99 (dd, J = 0.9 Hz, 8.7 Hz, 1H), 7.73 (dd, J = 6.9 Hz, 8.7 Hz, 1H), 4.51 (t, J = 7.2 Hz, 2H), 3.65 (t, J = 6.3 Hz, 2H), 2.05 (quint, J = 7.2 Hz, 2H), 1.60 (m, 2H), 1.45 (m, 4H). ^{13}C NMR (75 MHz, $CDCl_3$): δ (ppm) 155.6, 152.1, 143.3, 130.3, 125.7, 124.2, 123.7, 121.0, 62.9, 50.7, 32.6, 30.6, 26.5, 25.4. MS (ESI+) m/z (%): 304.1222 (15) $[M + H]^+$, 326.1044 (100) $[M + Na]^+$.

*4-(1-Dodecyl-1H-1,2,3-triazol-4-yl)benzo[c][1,2,5]thiadiazole (**21**).* 4-Ethynylbenzo[*c*][1,2,5]thiadiazole (**19**; 13.0 mg, 0.081 mmol, 1.0 equiv) was suspended in *tert*-butyl alcohol (1.1 mL). 1-Dodecyl azide (18.0 mg, 0.085 mmol, 1.05 equiv), an aqueous solution of $CuSO_4{\cdot}5H_2O$ (491.0 μL, 8.1 μmol, 0.1 equiv, from a 4.12 mg mL^{-1} solution in water) and an aqueous solution of sodium ascorbate (554.0 μL, 24.3 μmol, 0.3 equiv, from a 8.7 mg mL^{-1} solution in water) were then added. The resulting mixture was stirred at 110 °C under Ar for 30 h. The mixture was diluted with H_2O and extracted twice with DCM. The organic phase was dried over $MgSO_4$, filtered, and evaporated. The residue was purified by column chromatography on silica gel (eluent DCM) to afford 4-(1-dodecyl-1*H*-1,2,3-triazol-4-yl)benzo[*c*][1,2,5]-thiadiazole **21** as a colorless solid (24.0 mg, 80% chemical yield).

R_f (DCM/MeOH 98/2) = 0.74. ^{1}H NMR (300 MHz, $CDCl_3$): δ (ppm) 8.74 (s, 1H), 8.56 (dd, J = 0.9 Hz, 6.9 Hz, 1H), 7.97 (dd, J = 0.9 Hz, 8.7 Hz, 1H), 7.71 (dd, J = 6.9 Hz, 8.7 Hz, 1H), 4.48 (t, J = 7.2 Hz, 2H), 2.02 (quint, J = 7.2 Hz, 2H), 1.35 (m, 18H), 0.87 (t, J = 6.9 Hz, 3H). ^{13}C NMR (75 MHz, $CDCl_3$): δ (ppm) 155.4, 152.0, 143.2, 130.1, 125.5, 124.0, 123.8, 120.7, 50.7, 32.0, 30.5, 29.7, 29.6, 29.5, 29.4, 29.1, 26.6, 22.8, 14.2. HRMS (ESI+): calcd for $C_{20}H_{29}N_5NaS$ 394.2036, found 394.2040.

*[6-(4-(Benzo[c][1,2,5]thiadiazol-4-yl)-1H-1,2,3-triazol-1-yl)hexan-1-ol]bromotricarbonylrhenium(I) (**N**).* This compound was obtained according to general procedure B starting from 6-(4-(benzo[*c*][1,2,5]-thiadiazol-4-yl)-1*H*-1,2,3-triazol-1-yl)hexan-1-ol (**20**; 23.9 mg, 78.8 μmol, 1.0 equiv) after filtering, washing with toluene, and drying under vacuum as a bright orange solid (35.2 mg, 68% chemical yield).

^{1}H NMR (300 MHz, acetone-d_6): δ (ppm) 9.22 (s, 1H), 8.45 (dd, J = 0.9 Hz, 7.2 Hz, 1H), 8.26 (dd, J = 0.9 Hz, 9.0 Hz, 1H), 7.98 (dd, J = 7.2 Hz, 9.0 Hz, 1H), 4.71 (t, J = 7.2 Hz, 2H), 3.52 (t, J = 6.0 Hz, 2H), 2.10 (m, 2H), 1.52−1.44 (m, 6H). ^{13}C NMR (75 MHz, CD_3OD): δ (ppm) 155.5, 147.6, 142.0, 132.2, 129.9, 125.1, 124.6, 121.4, 62.7, 53.0, 33.3, 30.7, 27.1, 26.2. MS (ESI+) m/z (%): 574.0547 (100) $[M - Br]^+$, 675.9619 (80) $[M + Na]^+$. HRMS (ESI+): calcd for $C_{17}H_{17}BrN_5NaO_4ReS$ 675.9616, found 675.9619. HPLC (0 to 100% ACN in 30 min, column C8A): rt 19.96 (92.9%). IR: ν_{max}/cm^{-1} 2022, 1916, 1889 (CO).

*[4-(1-Dodecyl-1H-1,2,3-triazol-4-yl)benzo[c][1,2,5]thiadiazole]-bromotricarbonylrhenium(I) (**O**).* This compound was obtained according to general procedure B starting from 4-(1-dodecyl-1*H*-1,2,3-triazol-4-yl)benzo[*c*][1,2,5]thiadiazole (**21**; 10.4 mg, 28.0 μmol, 1.0 equiv) after purification by column chromatography on silica gel (cyclohexane/EtOAc 30/70) as a bright orange solid (16.0 mg, 79% chemical yield).

^{1}H NMR (300 MHz, d_6-acetone): δ (ppm) 9.22 (s, 1H), 8.46 (dd, J = 0.9 Hz, 7.2 Hz, 1H), 8.27 (dd, J = 0.9 Hz, 9.0 Hz, 1H), 8.00 (dd, J = 7.2 Hz, 9.0 Hz, 1H), 4.71 (t, J = 7.2 Hz, 2H), 2.10 (m, 2H), 1.44−1.26 (m, 18H), 0.86 (t, J = 7.2 Hz, 3H). ^{13}C NMR (75 MHz, CD_3OD): δ (ppm) 154.2, 146.3, 140.8, 130.6, 127.9, 124.2, 121.9, 120.1, 52.4, 32.0, 29.91, 29.85, 29.7, 29.6, 29.5, 29.0, 26.5, 22.8, 14.3. HRMS (ESI+): calcd for $C_{23}H_{29}BrN_5NaO_3ReS$ 744.0606, found 744.0591. HPLC (40 to 100% ACN in 20 min, column C18): rt 22.22 (97.5%). IR: ν_{max}/cm^{-1} 2040, 2026, 1936, 1918, 1897 (CO).

*4-Azidobenzo[c][1,2,5]thiadiazole (**22**).* 4-Aminobenzo[*c*][1,2,5]-thiadiazole (500.0 mg, 3.31 mmol, 1.0 equiv) was suspended in water (10.0 mL); concentrated aqueous HCl was added (1.0 mL), and the solution was cooled at 0 °C. A solution of $NaNO_2$ (274.0 mg, 3.97 mmol, 1.2 equiv) in water (1.5 mL) was added dropwise at 0 °C, and the mixture was further stirred for 20 min. A solution of NaN_3 (322.5 mg, 4.96 mmol, 1.5 equiv) in water (1.5 mL) was added dropwise at 0 °C, and the obtained suspension was stirred for 3 h. The solution was extracted with Et_2O; the organic phase was washed with saturated brine, dried over $MgSO_4$, filtered, and concentrated under reduced pressure. The residue was purified by column chromatography on silica gel (DCM) to afford 4-azidobenzo[*c*][1,2,5]thiadiazole (**22**) as a brown solid (150.0 mg, 26% chemical yield).

R_f (DCM) = 0.79. ^{1}H NMR (300 MHz, $CDCl_3$): δ (ppm) 7.35 (dd, J = 0.9, 8.7 Hz, 1H), 7.51 (dd, J = 1.2, 7.2 Hz, 1H), 7.09 (dd, J = 0.9, 7.5 Hz, 1H). ^{13}C NMR (75 MHz, $CDCl_3$): δ (ppm) 155.9, 149.1, 132.0, 129.7, 117.6, 116.5.

*4-(4-Dodecyl-1H-1,2,3-triazol-1-yl)benzo[c][1,2,5]thiadiazole (**23**).* This compound was obtained following general procedure A at 100 °C for 4 days starting from 4-azidobenzo[*c*][1,2,5]thiadiazole (**22**; 35.0 mg, 0.198 mmol, 1.0 equiv) and 1-tetradecyne (53.5 μL, 0.217 mmol, 1.1 equiv) after purification by column chromatography on silica gel (cyclohexane/EtOAc 85/15) as a pale yellow solid (41.0 mg, 56% chemical yield).

^{1}H NMR (300 MHz, $CDCl_3$): δ (ppm) 8.83 (s, 1H), 8.39 (d, J = 7.2 Hz, 1H), 8.05 (d, J = 8.7 Hz, 1H), 7.76 (t_{app}, J = 8.1 Hz, 1H), 2.86 (t, J = 7.5 Hz, 2H), 1.79 (quint, J = 7.5 Hz, 2H), 1.34 (m, 18H), 0.86 (t, J = 6.9 Hz, 3H). ^{13}C NMR (75 MHz, $CDCl_3$): δ (ppm) 155.9, 149.0, 146.8,

dx.doi.org/10.1021/ic5007007 | *Inorg. Chem.* 2014, 53, 6204−6223

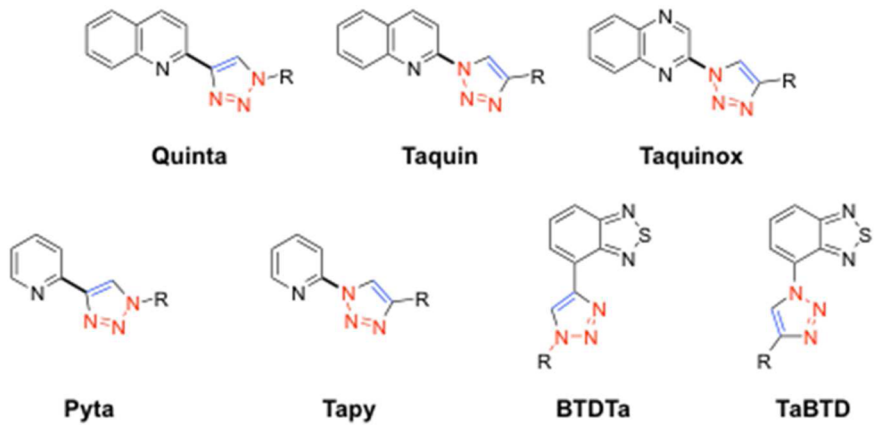

Figure 1. Structures of the ligands used in this study.

129.7, 128.8, 122.4, 121.2, 120.3, 32.0, 29.8, 29.77 (2C), 29.7, 29.5, 29.48 (2C), 29.4, 25.8, 22.8, 14.2.

*[4-(4-Dodecyl-1H-1,2,3-triazol-1-yl)benzo[c][1,2,5]thiadiazole]-bromotricarbonylrhenium(I) (**P**).* This compound was obtained according to general procedure B starting from 4-(4-dodecyl-1*H*-1,2,3-triazol-1-yl)benzo[*c*][1,2,5]thiadiazole (**23**; 8.1 mg, 27.0 μmol, 1.0 equiv) after purification by column chromatography on silica gel (cyclohexane/EtOAc 30/70) as a red solid (15.0 mg, 95% chemical yield).

R_f (cyclohexane/EtOAc 3/7) = 0.55. ^{1}H NMR (300 MHz, $CDCl_3$): δ (ppm) 8.33 (s, 1H), 8.19 (d, J = 8.7 Hz, 1H), 7.96 (d, J = 7.5 Hz, 1H), 7.40 (dd, J = 7.5, 8.7 Hz, 1H), 2.83 (m, 2H), 1.76 (quint, J = 7.5 Hz, 2H), 1.28−1.23 (m, 18H), 0.88 (t, J = 6.9 Hz, 3H). ^{13}C NMR (75 MHz, $CDCl_3$): δ (ppm) 155.2, 151.5, 142.3, 130.5, 126.7, 123.9, 120.5, 119.0, 32.1, 29.84, 29.81, 29.8, 29.7, 29.5, 29.4, 29.3, 28.7, 25.6, 22.8, 14.3. MS (ESI+) m/z (%): 744.0591 (24) $[M + Na]^+$, 393.2955 (100). HRMS (ESI+): calcd for $C_{23}H_{29}BrN_5NaO_3ReS$ 744.0606, found 744.0591. HPLC (40 to 100% ACN in 30 min, column C18A): rt 22.14 (>95%). IR: ν_{max}/cm^{-1} 2050, 2036, 1957, 1937, 1925, 1903 (CO).

X-ray Diffraction. X-ray crystallography was provided by the ICMMO in Orsay. Data were collected by using a Kappa X8 APPEX II Bruker diffractometer with graphite-monochromated Mo Kα radiation (λ = 0.71073 Å). Crystals were mounted on a CryoLoop (Hampton Research) with Paratone-N (Hampton Research) as cryoprotectant and then flash-frozen under a nitrogen gas stream at 100 K. The temperature of the crystal was maintained at the selected value (100 K) by means of a 700 series Cryostream cooling device to within an accuracy of ±1 K. The data were corrected for Lorentz−polarization and absorption effects. The structures were solved by direct methods using SHELXS-97[17a] and refined against F^2 by full-matrix least-squares techniques using SHELXL-97[17b] with anisotropic displacement parameters for all non-hydrogen atoms. Hydrogen atoms were located on a difference Fourier map and introduced into the calculations as a riding model with isotropic thermal parameters. All calculations were performed by using the Crystal Structure crystallographic software package WINGX.[17c]

After complex Re-Taquin-C4OH-Br (**F**) was dissolved in chloroform, yellow crystals suitable for X-ray diffraction were obtained upon slow evaporation of the solvent.

CCDC 983687 contains supplementary crystallographic data for this paper. These data can be obtained free of charge from the Cambridge Crystallographic Data Centre via http://www.ccdc.cam.ac.uk/Community/Requestastructure.

Crystal data: formula $C_{18}H_{16}BrN_4O_4Re$; molecular weight M_r = 621.48; monoclinic, space group $P2_1/n$; a = 7.3351(3) Å; b = 13.5173(7) Å; c = 19.1874(9) Å; α = 90.00°; β = 90.8520(10)°; γ = 90.00°; V = 1902.23 Å^3; T = 100(1) K; Z = 4; Z' = 0; μ(Mo Kα) = 8.522 mm^{-1}; 32913 reflections measured; 8302 unique data; 6832 reflections with $I > 22\sigma(I)$, $R(I > 2\sigma(I))$ = 0.0555.

Luminescence Quantum Yield Determination. Luminescence emission studies were performed on a Jasco FP-8300 spectrofluorometer. Emission spectra were recorded at two concentrations and for three different excitation wavelengths (at the absorption maximum λ_{abs}^{max} and around $\lambda_{abs}^{max} - 10$ and $\lambda_{abs}^{max} + 10$). The average integrated emission area F for the six measurements is used to determine the quantum yield in the equation

$$\phi_s = \phi_r\left(\frac{A_r}{A_s}\right)\left(\frac{F_s}{F_r}\right)\left(\frac{{n_s}^2}{{n_r}^2}\right)$$

where the subscripts s and r refer to the sample and the standard reference solution, respectively, n is the refractive index of the solvents, F is the integrated emission intensity, A is the absorbance at the excitation wavelength ($A < 0.1$), and ϕ is the luminescence quantum yield. Quinine sulfate in 0.1 N sulfuric acid was used as the standard with a known emission quantum yield of 0.546 (λ_{ex} 330−350 nm).

Conductivity Measurements. Measurements were performed with a CDM210 conductivity meter (Meter Lab, Radiometer Copenhagen). The cell was calibrated using a 0.1 M aqueous KCl solution with a conductance of 11.97 mS cm^{-1} at 21 °C. Solutions of compounds of interest were prepared at 10 μM in a H_2O/DMSO 95/5 mixture.

Computations. The calculations were performed using the Gaussian 09 program package. Geometries of all complexes were optimized for the singlet and triplet states with the DFT method using the hybrid B3LYP functional (unrestricted open-shell UB3LYP version for triplet states) and the 6-311G** basis set for all atoms except rhenium, for which the LANL2DZ basis set was used. Vibrational harmonic frequency analysis of the optimized geometries was used to ensure that there were true local minima with no imaginary frequencies.

The intensities of the 6 and 30 lowest-energy electronic transitions were calculated using the TD-DFT method with the UB3LYP functional, and the solvent effect was simulated using the polarizable continuum model (PCM) for water.

Cell Culture. MDA-MB-231 breast cancer cells obtained from the Human Tumour Cell Bank were used for the experiments. Cells were maintained in monolayer culture in DMEM (Dulbecco's Modified Eagle Medium) with phenol red/Glutamax I, supplemented with 9% of decomplemented fetal calf serum and 0.9% kanamycine, at 37 °C in a 5% CO_2 air humidified incubator. Both control and treated cells were processed in a similar way. They were seeded on glass slides (deposited in 35 × 10 mm Petri dishes) in order to reach confluency after 48 h at 37 °C under an atmosphere of 95% air/5% CO_2. The medium was removed, and fresh growth medium (1.5 mL of DMEM without phenol red and supplemented as previously described) was added to each flask of control cells. In the case of treated cells, 1.5 mL of a solution of a given compound in fresh growth medium (10 or 25 μM prepared from a 5 × 10^{-3} M stock solution in DMSO) was added. The cells were incubated at 37 °C under an atmosphere of 95% air/5% CO_2 for 1 h. The medium was then removed, and the cells were washed twice with

dx.doi.org/10.1021/ic5007007 | Inorg. Chem. 2014, 53, 6204−6223

Scheme 1. Synthesis of Taquinox and Taquin Complexes[a]

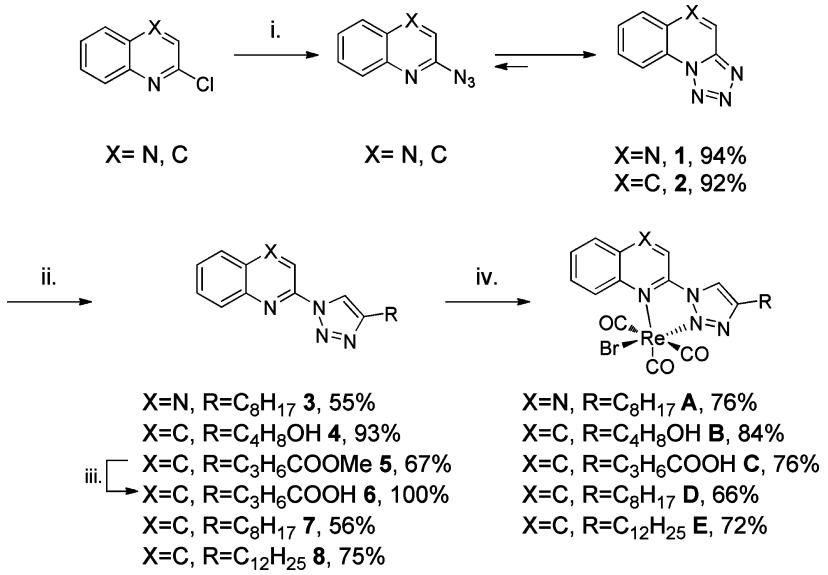

[a]Legend: (i) NaN_3, DMF/H_2O, 85 °C, 3 days; (ii) alkyne, $(CuOTf)_2.C_6H_6$, toluene, 100 or 110 °C; (iii) aqueous NaOH, acetone, 50 °C, 16 h; (iv) $Re(CO)_5Br$, toluene, 110 °C.

phosphate buffered saline (Dulbecco's PBS (D-PBS), 1X, 2 mL). Cells were fixed by 4% paraformaldehyde (PFA; 1.5 mL) for 8 min at room temperature and washed once with D-PBS (1X, 2 mL) and once with pure water (2 mL). Slides were mounted using Vectashield solution (H-1000, Vector Laboratories) just after the last water washing.

Fluorescence Imaging and Relative Cellular Uptake. In-cell fluorescence imaging was performed using an IX71 (Olympus) microscope equipped with a CCD (charged-coupled device, C-9100-02, Hamamatsu Corp., Sewickley, PA) and ×60 (Plan Apo, NA 1.42) objective. Compounds were detected using an appropriate filter set (excitation D350/50x; beam splitter 400DCLP; emission HQ560/80m; Chroma Technology) and excited using a Hg lamp (100 W) attenuated by a neutral density filter (ND-1). Microscope settings and functions were controlled using Simple PCI software (Hamamatsu). Image analysis was performed using ImageJ Software and Simple PCI software. For each image, the mean perinuclear luminescence intensity per cell corrected for the background was determined (using ImageJ software). For each condition (10 or 25 μM), average values and error bars were calculated over a number of cells indicated directly below the corresponding histogram in Figure 17 (right).

RESULTS AND DISCUSSION

Design and Synthesis of New Rhenium Complexes. We investigated the impact of structural modifications of the bidentate ligand coordinating the rhenium(I) ion on the luminescent properties of the complexes. We first focused on modifications of the Pyta ligand and its extended version containing a quinoline ring instead of a pyridine thereafter named Quinta. We investigated the influence of inverting the bridge between the heterocycle and the triazole ring. In the parent Pyta and Quinta series, the triazole ring is formed by reaction between the alkyne-functionalized heterocycle and an azido side chain. We synthesized here a series of ligands in which the triazole ring is linked to the heterocycle (pyridine, quinoline, or quinoxaline) by a nitrogen atom (Figure 1) and systematically compared the physicochemical properties of the $Re(CO)_3$ associated complexes with those of the corresponding parent compounds.

Unlike the Tapy ligand (1-(2-pyridyl)-1,2,3-triazole), which has been quite documented in the literature, very few

Scheme 2. Synthesis of Quinta Complexes[a]

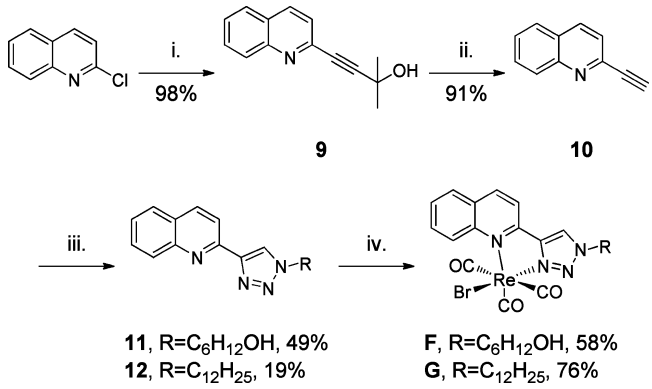

[a]Legend: (i) 2-methylbut-3-yn-2-ol, $Pd(PPh_3)_2Cl_2$, CuI, Et_2NH, 40 °C, 30 min; (ii) NaOH (0.1 equiv), toluene, reflux, 1 h; (iii) azide derivative, $CuSO_4{\cdot}5H_2O$, sodium ascorbate, tBuOH/H_2O, 110 °C; (iv) $Re(CO)_5Br$, toluene, 110 °C.

references[8,18] can be found that describe compounds incorporating respectively the 1-(quinolin-2-yl)-1,2,3-triazol-4-yl ligand (Taquinox) and the 1-(quinolin-2-yl)-1,2,3-triazol-4-yl ligand (Taquin) (Figure 1). Moreover, no metal complex prepared from Taquin or Taquinox has been described and only very few complexes of Ru(II), Pd(II), or Pt(II) incorporating the Tapy ligand have been reported in the literature.[19] The coordination properties of these ligands have thus been overlooked, and the present paper describes, to the best of our knowledge, the first rhenium tricarbonyl complexes incorporating such ligands in their coordination sphere.

We first synthesized quinoxaline- and quinoline-based complexes bearing various side chains. The synthesis was performed in three steps from the 2-chloro heterocycle derivatives (Scheme 1). Reaction of the starting materials with sodium azide in a refluxing mixture of DMF and water afforded in good yields the 2-azido derivatives, which exist in equilibrium with the tetrazolo derivatives **1** and **2**, as discussed by Chattopadhyay et al.[8] These unsubstituted tetrazoles are

dx.doi.org/10.1021/ic5007007 | Inorg. Chem. 2014, 53, 6204−6223

Scheme 3. Synthesis of Tapy Complexes[a]

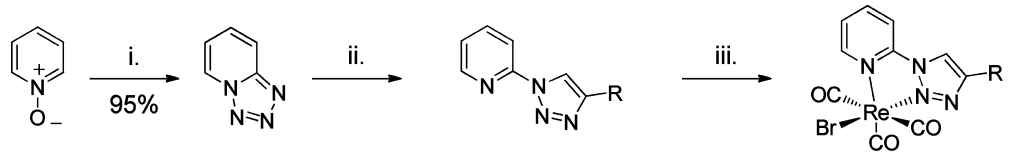

[a]Legend: (i) diphenylphosphoryl azide (DPPA), pyridine, 120 °C, 24 h; (ii) alkyne, $(CuOTf)_2{\cdot}C_6H_6$, toluene, 110 °C; (iii) $Re(CO)_5Br$, toluene, 110 °C.

Scheme 4. Synthesis of Tapy Complex L[a]

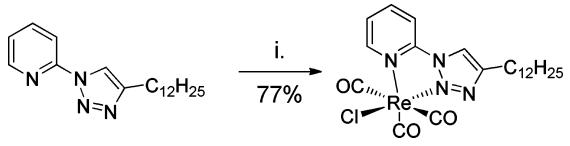

[a]Legend: (i) $Re(CO)_5Cl$, toluene, 110 °C.

expected to predominantly exist in the closed form.[8] With this kind of pyridotetrazole derivative, Cu-catalyzed azide alkyne cycloadditions (CuAAC) are generally unsuccessful under standard conditions. Therefore, to perform the desired click reactions between the quinoxalino- and quinolinotetrazoles **1** and **2** and various alkynes, we applied a previously reported procedure using Cu(I) trifluoromethanesulfonate benzene complex as a catalyst in toluene.[8] Reactions were performed in a sealed tube under an inert atmosphere to avoid oxidation of the catalyst, and heating appeared necessary for the reactions to proceed. All of the alkynes used were commercially available except for methyl hex-5-ynoate, necessary to prepare ligand **5**, which was synthesized in two steps from hexyn-1-ol by Jones oxidation followed by esterification.[12] Ligand **5** was quantitatively hydrolyzed under basic conditions to afford **6** prior to rhenium coordination. Coordination of the ligands **3**, **4**, and **6**–**8** with rhenium was achieved by reaction with rhenium pentacarbonyl bromide in refluxing toluene to afford complexes **A**–**E** in good yields (Scheme 1).

Butanol and butanoic side chains were chosen, as they enable further chemical modifications of the terminal functional group or grafting of the ligand on other moieties of interest. We also introduced aliphatic side chains of different lengths in order to investigate the impact of increasing alkyl chain length and hydrophobic character on the optical properties, as already described for other rhenium tricarbonyl complexes.[20]

To assess the influence of the inversion of the triazole link to the heterocycle, two rhenium complexes of the Quinta series have been synthesized bearing either a side chain terminated by the primary alcohol (**F**) or a 12-carbon alkyl chain (**G**) (Scheme 2). 2-Ethynylquinoline (**10**) was prepared from 2-chloroquinoline by a Sonogashira coupling with 2-methylbut-3-yn-2-ol in the presence of CuI and bis(triphenylphosphine)palladium(II) dichloride followed by treatment with a catalytic amount of solid NaOH in refluxing toluene.[9] The Quinta ligands **11** and **12** were then prepared by CuAAC "click" reactions under classical conditions (Scheme 2) with azidohexanol[14a] or dodecyl azide[14b] previously prepared according to described procedures. The complexes **F** and **G** were finally formed after reaction with rhenium pentacarbonyl bromide as above.

A series of four pyridine-based ligands (Tapy derivatives) bearing either a butanol or an aliphatic side chain of variable length ($R = -C_nH_{2n+1}$, n = 4, 8, 12) and their corresponding rhenium complexes **H**–**K** were synthesized using the same strategy from the tetrazolopyridine **13** (Scheme 3). This intermediate was prepared in high yield by treatment of pyridine *N*-oxide by diphenylphosphoryl azide in pyridine at 120 °C for 24 h.

All of the Re(I) tricarbonyl complexes described at this stage were synthesized using the rhenium pentacarbonyl bromide precursor and thus have a bromide as ligand. In order to study the potential influence of this halide ligand and to compare their properties with those of Re-Pyta-C12-Cl described elsewhere,[20b] we prepared complex **L** bearing a chloride ligand instead of a bromide (Scheme 4). Complex **L** was prepared from ligand **17** by reaction with rhenium pentacarbonyl chloride in toluene at 110 °C.

Scheme 5. Synthesis of BTDTa Complexes[a]

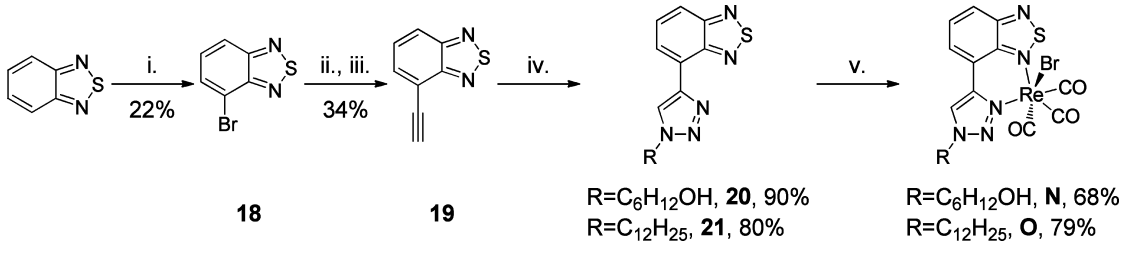

[a]Legend: (i) Br_2, HBr 33%, AcOH; (ii) TMSA, CuI, $Pd(PPh_3)_2Cl_2$, Et_3N/DMF; (iii) K_2CO_3, MeOH; (iv) azide, $CuSO_4{\cdot}5H_2O$, sodium ascorbate, $tBuOH/H_2O$; (v) $Re(CO)_5Br$, toluene, 110 °C.

dx.doi.org/10.1021/ic5007007 | Inorg. Chem. 2014, 53, 6204–6223

Scheme 6. Synthesis of TaBTD Complex[a]

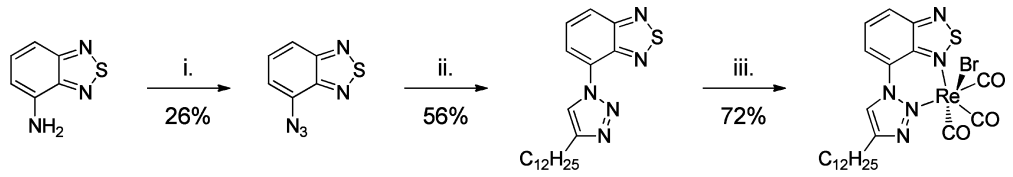

22 23 P

[a]Legend: (i) $NaNO_2$, NaN_3, aqueous HCl, (ii) tetradecyne, $(CuOTf)_2.C_6H_6$, toluene, 110 °C; (iii) $Re(CO)_5Br$, toluene.

Table 1. Nomenclature Used for the Complexes A–P

complex	letter	aromatic ligand[a]	side chain	X ligand
Re-Taquinox-C8-Br	**A**	Taquinox	$-C_8H_{17}$	Br
Re-Taquin-C4OH-Br	**B**	Taquin	$-C_4H_8OH$	Br
Re-Taquin-C3COOH-Br	**C**	Taquin	$-C_3H_6COOH$	Br
Re-Taquin-C8-Br	**D**	Taquin	$-C_8H_{17}$	Br
Re-Taquin-C12-Br	**E**	Taquin	$-C_{12}H_{25}$	Br
Re-Quinta-C6OH-Br	**F**	Quinta	$-C_6H_{12}OH$	Br
Re-Quinta-C12-Br	**G**	Quinta	$-C_{12}H_{25}$	Br
Re-Tapy-C4OH-Br	**H**	Tapy	$-C_4H_8OH$	Br
Re-Tapy-C4-Br	**I**	Tapy	$-C_4H_9$	Br
Re-Tapy-C8-Br	**J**	Tapy	$-C_8H_{17}$	Br
Re-Tapy-C12-Br	**K**	Tapy	$-C_{12}H_{25}$	Br
Re-Tapy-C12-Cl	**L**	Tapy	$-C_{12}H_{25}$	Cl
Re-Pyta-C12-Cl[19b]	**M**	Pyta	$-C_{12}H_{25}$	Cl
Re-BTDTa-C6OH-Br	**N**	BTDTa	$-C_6H_{12}OH$	Br
Re-BTDTa-C12-Br	**O**	BTDTa	$-C_{12}H_{25}$	Br
Re-TaBTD-C12-Br	**P**	TaBTD	$-C_{12}H_{25}$	Br

[a]See Figure 1.

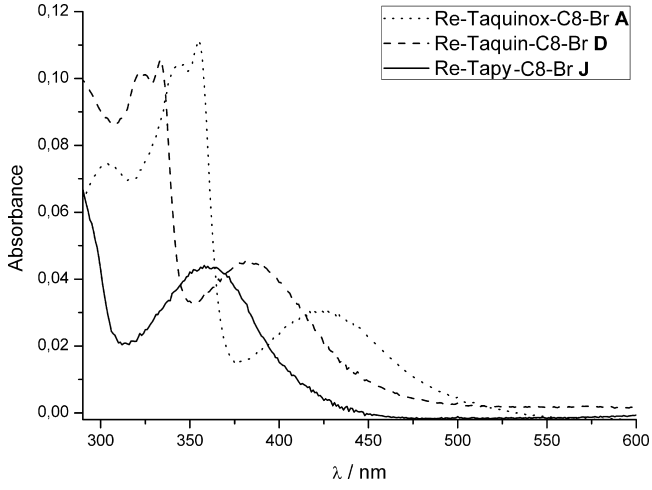

Figure 3. Absorption spectra of complexes **A**, **D**, and **J** in acetonitrile (10 μM).

We extended the series of rhenium complexes with benzothiadiazole–triazole-based compounds.[21] Both 4-(1-*R*-1*H*-1,2,3-triazol-4-yl)benzo[*c*][1,2,5]thiadiazole (BTDTa) and 4-(4-*R*-1*H*-1,2,3-triazol-1-yl)benzo[*c*][1,2,5]thiadiazole (TaBTD) containing $Re(CO)_3$ complexes were prepared. The synthesis of BTDTa complexes **N** and **O** was performed in five steps (Scheme 5). Monobrominated benzothiadiazole **18** was obtained in poor yield from the commercially available

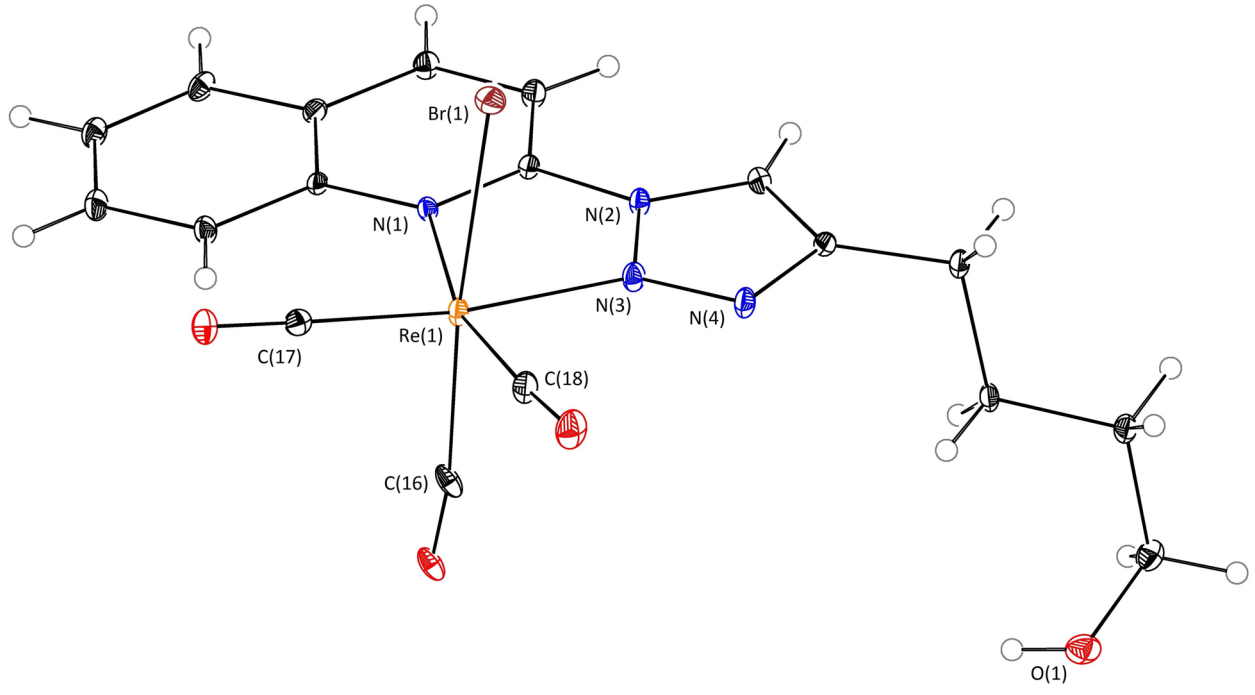

Figure 2. ORTEP drawing of Re-Taquin-C4OH-Br (**F**) (30% probability level).

dx.doi.org/10.1021/ic5007007 | *Inorg. Chem.* 2014, 53, 6204–6223

Table 2. Photophysical Data for the Complexes at Room Temperature in Acetonitrile

complex	letter	excitation (nm)	emission (nm)	range (nm)	yield (%)[a]	SD
Re-Taquinox-C8-Br	**A**					
Re-Taquin-C4OH-Br	**B**	380	617	515−700	0.05	0.01
Re-Taquin-C3COOH-Br	**C**	380	617	515−700	0.06	0.01
Re-Taquin-C8-Br	**D**	380	617	515−700	0.06	0.004
Re-Taquin-C12-Br	**E**	380	617	515−700	0.06	0.01
Re-Quinta-C6OH-Br	**F**					
Re-Quinta-C12-Br	**G**					
Re-Tapy-C4OH-Br	**H**	360	564	485−695	0.15	0.01
Re-Tapy-C4-Br	**I**	360	564	480−695	0.16	0.008
Re-Tapy-C8-Br	**J**	360	564	480−695	0.17	0.015
Re-Tapy-C12-Br	**K**	360	564	480−695	0.17	0.008
Re-Tapy-C12-Cl	**L**	360	569	485−695	0.19	0.009
Re-PyTa-C12-Cl[19b]	**M**	332	522	440−650	0.10	0.04
Re-BTDTa-C6OH-Br	**N**	365	470	400−560	0.53	0.06
Re-BTDTa-C12-Br	**O**	365	470	400−560	0.51	0.1
Re-TaBTD-C12-Br	**P**	355	455	395−560	0.99	0.09

[a]Determined relative to quinine sulfate (Φ = 54.6%) in 0.1 N H_2SO_4 as a standard. Differences in the refractive indices of the solvent systems were accounted for.

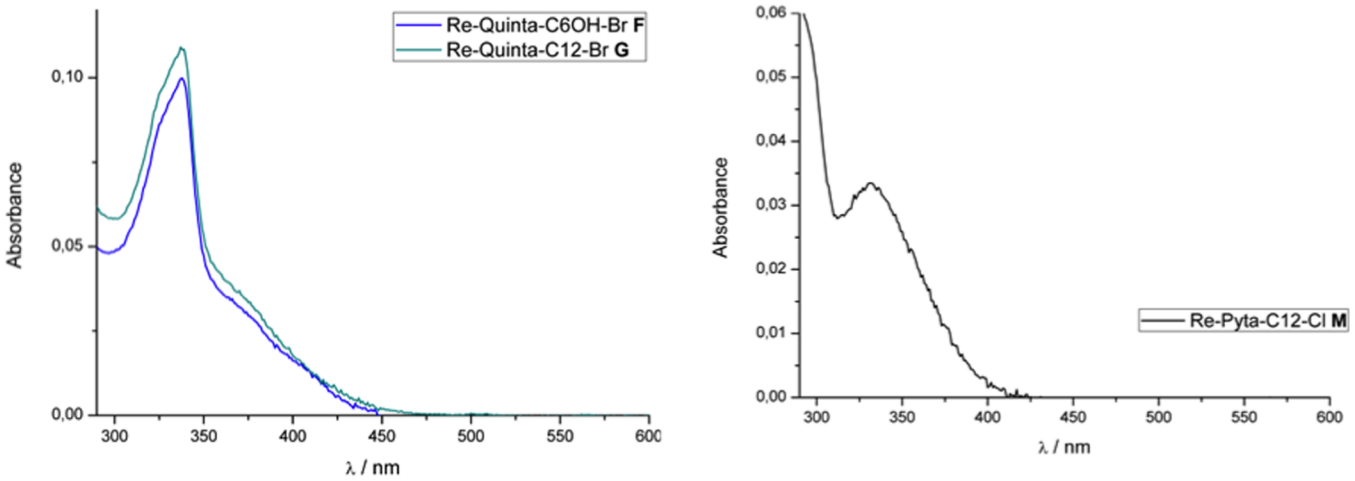

Figure 4. Absorption spectra of complexes **F** and **G** (left) and Re-Pyta-C12-Cl (**M**) (right) in acetonitrile (10 μM).

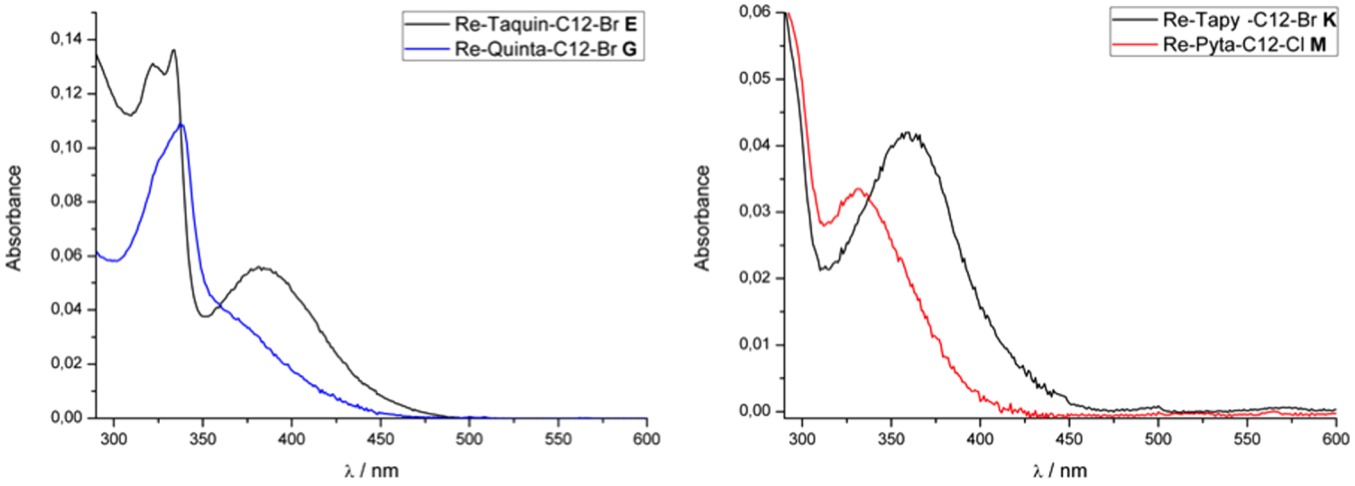

Figure 5. Absorption spectra of complexes **E** and **G** (left) and of complexes **K** and **M** (right) in acetonitrile (10 μM).

benzothiadiazole. Under the conditions used, the derivative dibrominated at positions 4 and 8 was mainly formed. Sonogashira coupling with (trimethylsilyl)acetylene (TMSA) followed by TMS deprotection under basic conditions afforded compound **19** in 34% yield over two steps. The ligands **20** and **21** were then prepared in good yields by CuAAC "click"

dx.doi.org/10.1021/ic5007007 | *Inorg. Chem.* 2014, 53, 6204−6223

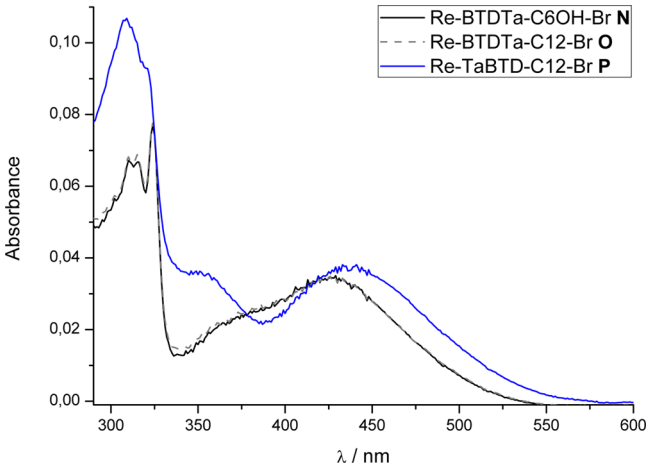

Figure 6. Absorption spectra of complexes **N**–**P** in acetonitrile (10 μM).

reactions with azidohexanol or dodecyl azide as mentioned above. The complexes **N** and **O** were finally formed after reaction with rhenium pentacarbonyl bromide.

Finally, the TaBTD complex **P** bearing a long C12 alkyl chain was synthesized using the same procedure used for the other inverted-bridge ligands described above, as shown in Scheme 6. The starting 4-azidobenzothiadiazole **22** was prepared from 4-aminobenzothiadiazole under classical azidation conditions.

For the sake of clarity in the following discussion, a systematic nomenclature will be used for the Re complexes as follows: Re-aromatic ligand-side chain-X ligand. All of the complexes described and studied here are summarized with their systematic names in Table 1.

Crystallography. We obtained crystals of the complex Re-Taquin-C4OH-Br (**F**) from chloroform solution under ambient conditions and performed X-ray analysis (Figure 2). The complex crystallizes in space group $P2_1/n$. The rhenium ion displays a distorted-octahedral coordination geometry. The bond lengths and angles are found in a range comparable to those for rhenium tricarbonyl complexes based on Pyta ancillary ligands (Supporting Information, Table S1).[5f] The rhenium atom is coordinated to two nitrogens of the Taquin ligand, one bromine atom, and three carbonyl groups in a *fac* geometry. The average Re–carbon bond length is 1.96 Å, and the OC–Re–CO angles are in the 88.7–95.2° range. The trans bond angles are respectively 165.7(2), 172.7(2), and 175.1(2)°, showing a moderate distortion in the octahedral geometry. The N(1)–Re(1)–N(3) angle has a value of 73.3(2)°, comparable to that found for Pyta-based Re complexes[5f] and reflecting the constrained five-membered coordination ring. Finally, the Taquin ligand in the Re–tricarbonyl complex is close to planar, with an angle between the planes defined by the two aromatic heterocycles (quinolinyl and triazolyl) of 5.92°.

Optical Properties of the Rhenium Complexes. We investigated the UV–vis and luminescence properties of the synthesized complexes. We first recorded spectra in acetonitrile at 10 μM concentrations. Rhenium complex **A** shows a structured band with two peaks around 345 and 355 nm and a broad band centered at 425 nm (Figure 3). The Taquin complexes **B**–**E** exhibit similar features with a blue shift: two peaks around 323 and 333 nm and a broad band centered at 380 nm (Figure 3, with **D** as a typical trend, and Table 2).

Quinta complexes **F** and **G** in acetonitrile exhibit a band centered at 338 nm and a shoulder around 375 nm that most likely have a significant metal to ligand charge transfer (MLCT) character. Re-Pyta-C12-Cl (**M**) shows a band centered at 288 nm ($\pi \rightarrow \pi^*$ intraligand transition) and a lower-energy band at 332 nm with MLCT character (Figure 4).[5c,d]

Complexes of the Tapy series **H**–**L** with a bromide or chloride as ligand show a band at 270 nm assigned to a $\pi \rightarrow \pi^*$ intraligand transition by analogy with Pyta complexes and a lower-energy band centered at 360 nm with MLCT character (Figure 3, exemplified by **J**, and Table 2). For the four series Quinta, TaQuin, Pyta, and Tapy described so far, the complexes of a same series have the same absorption profile in acetonitrile (organic solvent) whatever the nature of the appended side chain, as already pointed out in previous studies for comparable complexes.[20b,c] A significant impact of the small structural modification of inverting the bridge between the triazole ring and the heterocycle can be seen in the pyridine and quinoline series: in both pyridine and quinoline series, inverting the triazole bridge decreases the energy of the MLCT band: i.e., leads to a shift toward higher wavelengths (Figure 5). Finally, going from Tapy to Taquin to Taquinox ligand (Figure 3), i.e. extending the aromatic surface and/or the electron-deficient character of the heterocycle, leads also, as expected, to a bathochromic shift of the lowest-energy band.

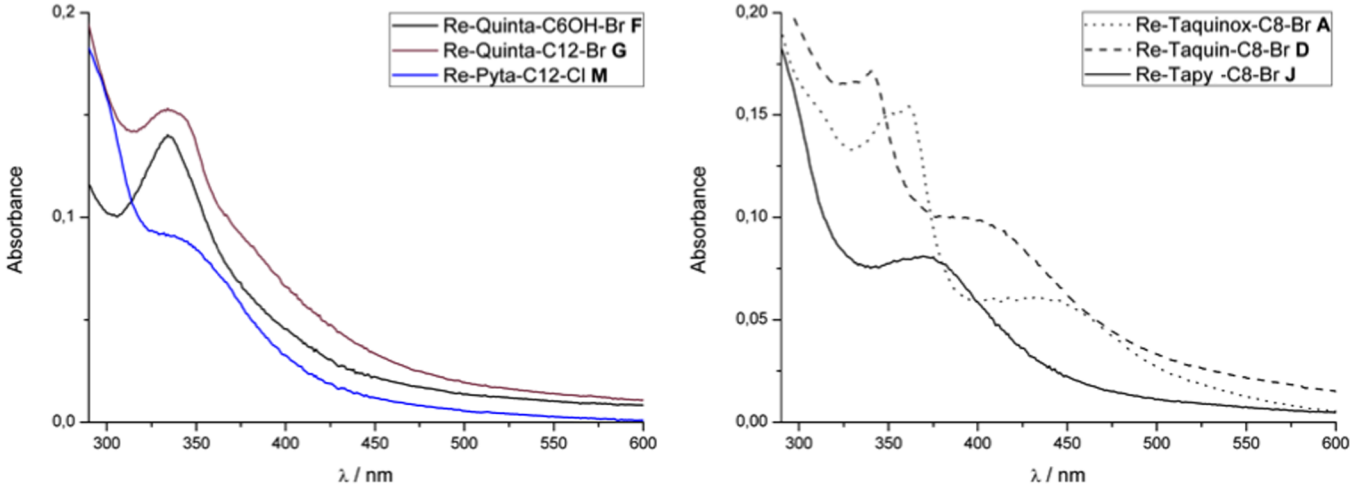

Figure 7. Absorption spectra of complexes **F**, **G**, and **M** (left) and of complexes **A**, **D**, and **J** (right) in H_2O/DMSO 98/2 (10 μM).

dx.doi.org/10.1021/ic5007007 | *Inorg. Chem.* 2014, 53, 6204–6223

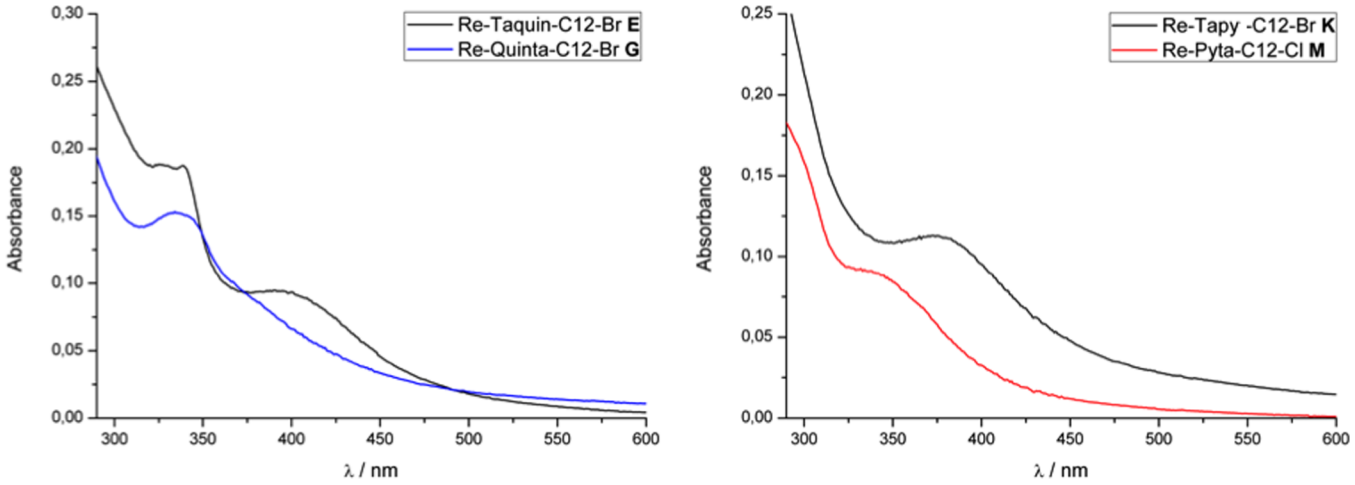

Figure 8. Absorption spectra of complexes **E** and **G** (left) and of complexes **K** and **M** (right) in H_2O/DMSO 98/2 (10 μM).

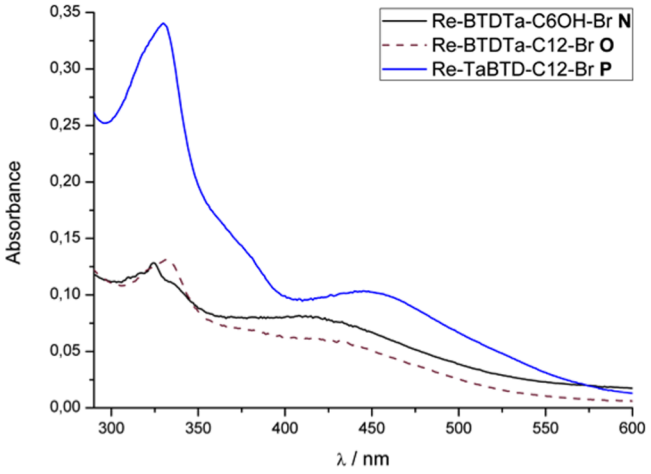

Figure 9. Absorption spectra of complexes **N**–**P** in H_2O/DMSO 98/2 (10 μM).

In the benzo[*c*][1,2,5]thiadiazole (BTD) series **N**–**P**, absorption profiles of complexes **N** and **O** show similar features (Figure 6): a structured peak at 324 nm, a shoulder at 365 nm with a MLCT character, and a broad absorption band centered at 420 nm. Going to the TaBTD series (from **O** to **P**) results only in slight changes in the absorption profile. The complex **P** exhibits a peak around 330 nm, a weak MLCT band at 355 nm, which is slightly blue-shifted in comparison to that for complex **O**, and a broad band at 435 nm.

We performed similar studies in aqueous solutions containing 2% DMSO, a better match for further biological studies. The absorption profiles of the Quinta complexes and of the Pyta complex are again comparable to those previously reported in the literature.[5b,6] Complexes **F** and **G** exhibit a band centered at 335 nm that most likely has a significant metal to ligand charge transfer (MLCT) character. Complex **M** shows a MLCT band centered at 340 nm (Figure 7, left).

Rhenium complex **A** shows a structured band with two peaks around 350 and 360 nm and a broad band centered at around 440 nm of undefined character. Under aqueous conditions, whereas the Taquin complexes **B**–**E** have similar absorption profiles, a strong impact of the side chain on the absorption maxima is observed. The complexes of the Tapy series **H**–**K**

Table 3. Photophysical Data for Complexes A–P at Room Temperature in a 98/2 H_2O/DMSO Mixture

complex	letter	excitation (nm)	emission (nm)	range (nm)	yield[a] (%)	SD
Re-Taquinox-C8-Br	**A**	360	648	555–790	0.08	0.01
Re-Taquin-C4OH-Br	**B**	375	610	515–750	0.26	0.02
Re-Taquin-C3COOH-Br	**C**	375	610	515–750	0.23	0.05
Re-Taquin-C8-Br	**D**	385	597	515–750	1.14	0.18
Re-Taquin-C12-Br	**E**	385	593	515–750	1.30	0.19
Re-Quinta-C6OH-Br	**F**	335	575	500–745	0.21	0.02
Re-Quinta-C12-Br	**G**	335	582	500–730	0.56	0.08
Re-Tapy-C4OH-Br	**H**	350	560	476–695	0.99	0.46
Re-Tapy-C4-Br	**I**	350	560	470–690	0.80	0.33
Re-Tapy-C8-Br	**J**	375	554	470–690	3.39	0.29
Re-Tapy-C12-Br	**K**	380	554	470–690	3.20	0.57
Re-Tapy-C12-Cl	**L**	370	554	470–690	3.56	0.22
Re-Pyta-C12-Cl	**M**	340	512	440–650	0.75	0.12
Re-BTDTa-C6OH-Br	**N**	340	495	425–580	0.05	0.02
Re-BTDTa-C12-Br	**O**					
Re-TaBTD-C12-Br	**P**					

[a]Determined relative to quinine sulfate (Φ = 54.6%) in 0.1 N H_2SO_4 as a standard. Differences in the refractive indices of the solvent systems were accounted for.

dx.doi.org/10.1021/ic5007007 | *Inorg. Chem.* 2014, 53, 6204–6223

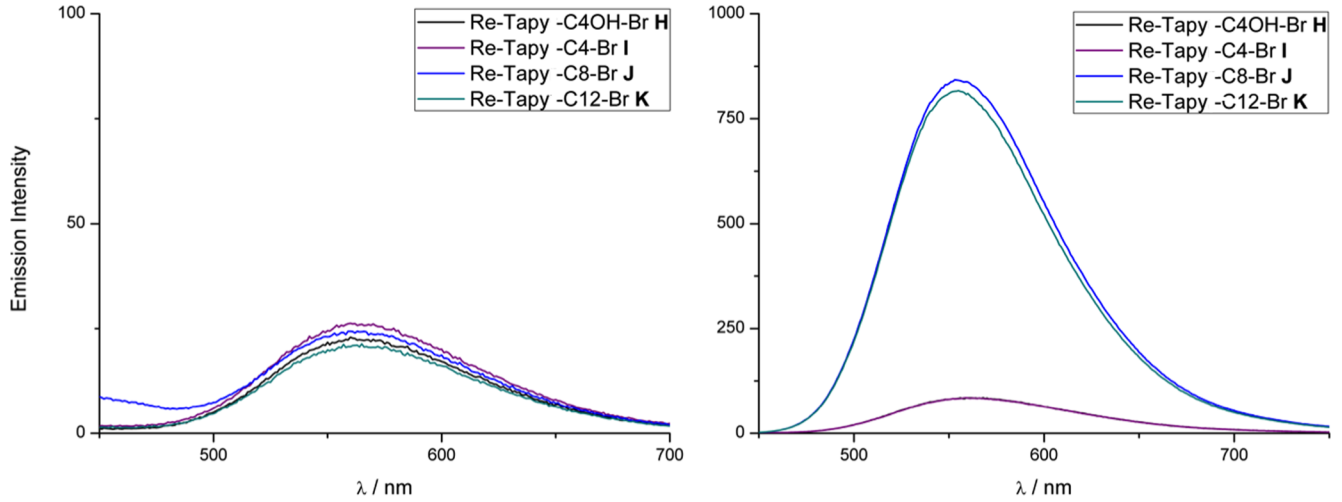

Figure 10. Luminescence emission spectra of Tapy complexes **H**−**K** (10 μM) in acetonitrile (left) and in H_2O/DMSO 98/2 (right) (λ_{exc} 370 nm).

share the same behavior, and this will be discussed in more detail below. Complexes **A**, **D**, and **J** bearing the same C8 side chain are thus compared. Complex **D** exhibits a structured band around 330 and 340 nm and a broad band centered at 380 nm. Tapy complex **J** shows a band at 290 nm assigned to a $\pi \rightarrow \pi^*$ intraligand transition by analogy with Pyta complexes and a lower-energy band centered at 380 nm with MLCT character (Figure 7, right). A significant impact of the bridge inversion is also evidenced in aqueous solution for the pyridine and quinoline series, and the same modifications in the absorption profiles as in acetonitrile can be observed (Figure 8). In aqueous solution, in the Tapy series, substituting the bromide ligand by a chloride (complex **K** to **L**) leads to a 10 nm blue shift of the MLCT band (from 380 to 370 nm), in contrast to what is observed in organic solvent.

In the BTD series, the BTDTa-based complexes **N** and **O** show a peak centered around 330 nm and a broad band around 415 nm (Figure 9, Table 3). In contrast to the case for acetonitrile and to the other series described in water, the absorption profiles do not significantly change upon modification of the side chain under aqueous conditions. Going to the TaBTD series (from **O** to **P**) results in deep changes in the absorption intensity. The complex **P** exhibits a peak around 330 nm with an ill-defined shoulder around 378 nm. A broad band is also observed centered at 450 nm, blue-shifted by 35 nm in comparison to complex **O**, a shift comparable with those observed for the other series (Figure 9, Table 3).

We then studied the emission properties of the rhenium complexes **A**−**P** at 10 μM both in acetonitrile and in a water/DMSO 98/2 mixture. Taquinox complex **A** appears to be nonemissive in acetonitrile upon photoexcitation at either 355 or 425 nm. Upon photoexcitation (λ_{exc} 380 nm), Taquin complexes **B**−**E** display broad emission bands centered at 617 nm of similar low intensities, whatever the nature of the side chain (Table 2). In comparison, the Quinta complexes **F** and **G** are essentially non emissive in acetonitrile. The Tapy complexes **H**−**K** display a broad emission band at 564 nm. Complex **L**, bearing a chloride ligand instead of a bromide, has a maximum emission at 569 nm. The Pyta complex **M** shows a typical broad emission band at 522 nm, in total agreement with data already reported for this complex or others of the family.[6] Inversion of the bridge between the triazole ring and the pyridine in the ligand induces a red shift of approximately 30−35 nm in the emission of their corresponding rhenium tricarbonyl complexes, while their Stokes shift remains high (190−205 nm). In all cases, the emissions most likely originate from a triplet ^{3}MLCT state as for related rhenium tricarbonyl complexes.

When the Pyta/Quinta and Tapy/Taquin series are compared, a red shift is observed in the emission of the quinoline-based complexes relative to the pyridine complexes, which fits previous records. Table 2 summarizes photophysical data for rhenium complexes **A**−**P** in acetonitrile along with the determined quantum yield values. In acetonitrile, the quantum yields obtained within a series are closely similar, whatever the nature of the appended side chain. Quantum yields for the quinoline-containing complexes **B**−**G** are dramatically low with a mean value of 0.06%. The Tapy complexes **H**−**L** have quantum yield values between 0.15 and 0.19%, slightly higher than the values for the Pyta complexes.

Surprisingly, BTD-based complexes **N**−**P** show narrower emission bands with higher intensities centered at 470 nm for **N** and **O** and 455 nm for **P**. The TaBTD series is characterized by a blue shift in emission in comparison with the BTDTa complexes, which is in opposition to the pyridine and quinoline families. Complexes **N**−**P** display also interesting quantum yield values in acetonitrile of 0.53, 0.51, and 0.99%, respectively, and may thus constitute a promising class of new rhenium probes in organic media.

The same experiments were then performed at the same concentration in water (2% DMSO). Upon photoexcitation at 360 nm, Taquinox complex **A** displays a low-intensity emission band at 647 nm. For the quinoline and pyridine families, trends similar to those in acetonitrile can be observed for the shifts in the maximum emission wavelengths. However, deep changes in emission intensities are observed in aqueous medium depending on the nature of the side chain for the Taquin and Tapy complexes. This behavior, which was already reported for Re-Pyta complexes with alkyl side chains of increasing length and for cationic rhenium complexes with a 2,2′-bipyridine and a lipophilic derivative of hydroxymethylpyridine as ligands,[20b,c] will be discussed in more detail below. The Taquin complexes **B**−**E** display broad emission bands between 593 and 610 nm depending on the side chain (vide infra). These bands are blue-shifted in comparison with the emission of quinoxaline derivative **A** and slightly red-shifted in comparison to the Quinta analogues **F** and **G**, which show maximum emissions at

dx.doi.org/10.1021/ic5007007 | Inorg. Chem. 2014, 53, 6204−6223

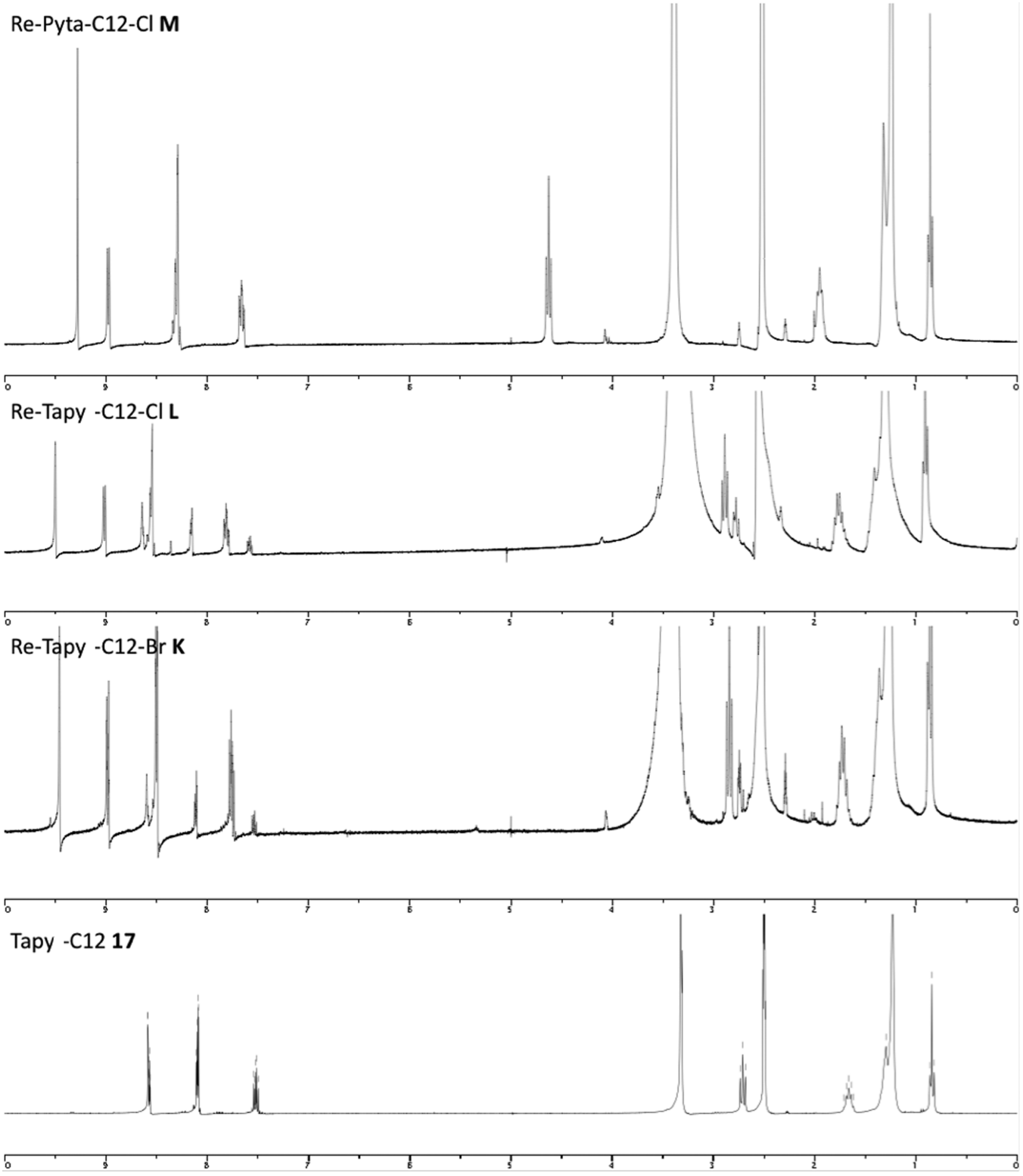

Figure 11. Stacked ^{1}H NMR spectra of complexes **M**, **L**, and **K** ($c \approx 5.0$ mg/mL) and ligand **17** in d_6-DMSO after 4 days.

575 and 582 nm, respectively, close to published values for similar complexes.[5b] The Tapy complexes **H**−**L** display a broad emission band at 560 or 554 nm depending on the side chain (vide infra). The Pyta complex **M** shows a typical broad emission band at 512 nm, in total agreement with data already reported for this complex or other closely related species.[7] Inversion of the bridge between the triazole ring and the pyridine in the ligand induces a bathochromic shift of approximately 45−50 nm in the emission of their corresponding rhenium tricarbonyl complexes. In all cases again, the emissions most likely originate from a triplet ^{3}MLCT state as for related rhenium tricarbonyl complexes.[5d−f,6] When the Pyta/Quinta and Tapy/Taquin series are compared, a red shift is observed in the emission of the quinoline-based complexes relative to the

dx.doi.org/10.1021/ic5007007 | *Inorg. Chem.* 2014, 53, 6204−6223

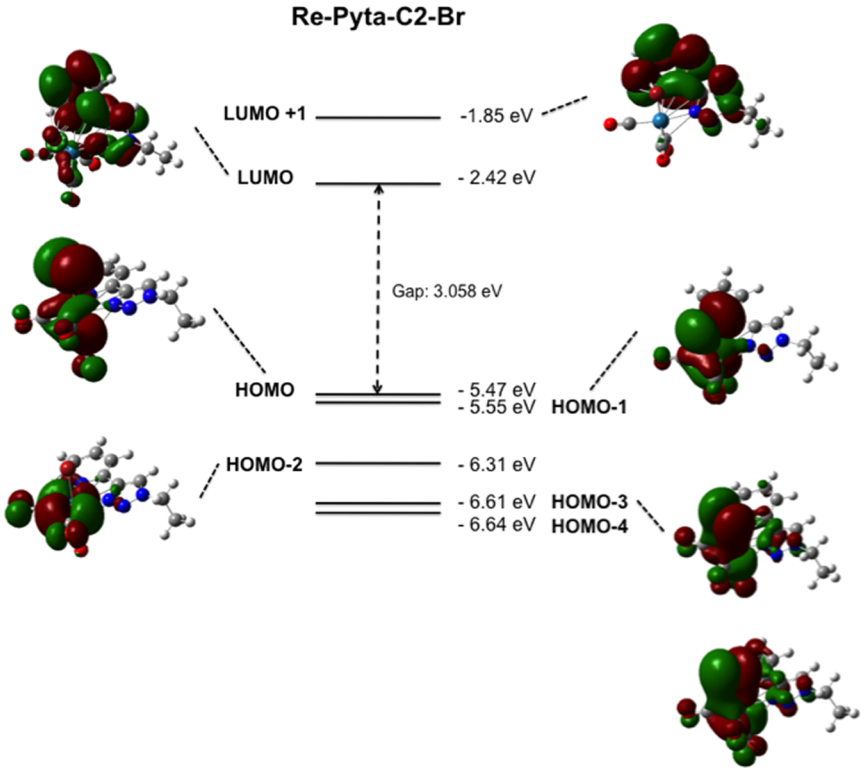

Figure 12. Frontier orbital diagram for Re-Pyta-C2-Br.

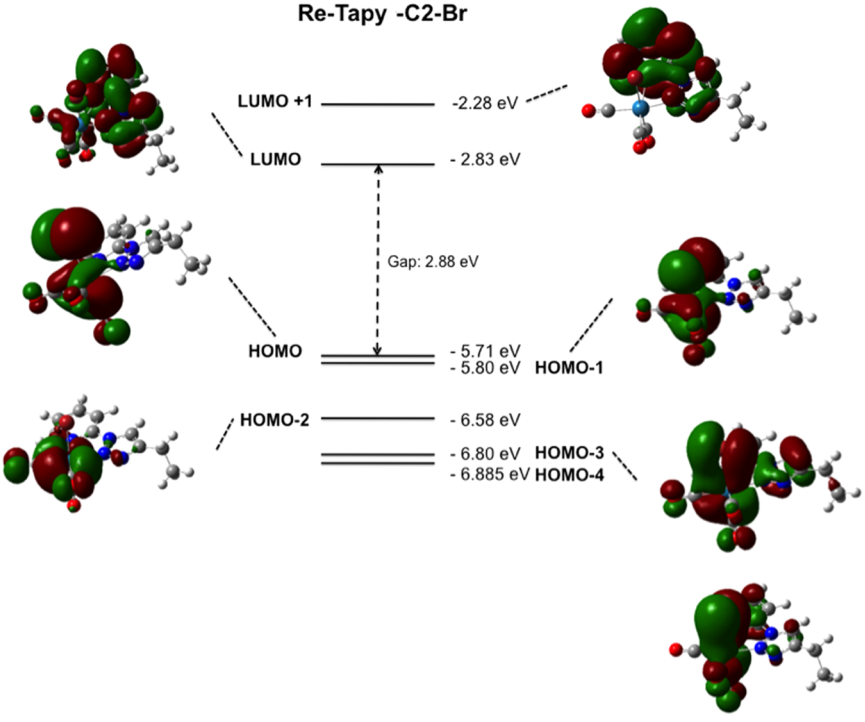

Figure 13. Frontier orbital diagram for Re-Tapy-C2-Br.

pyridine complexes, which fits previous records and fits those observed in organic solvent. Surprisingly, BTD-based complexes **N**−**P** are overall nonemissive, whatever the excitation wavelength in aqueous solution.

A direct comparison of complex **E** with **G** and **L** with **M** highlights the huge impact of the bridge inversion alone on the photophysical properties of rhenium tricarbonyl complexes bearing long alkyl chains in aqueous medium. Quantum yield values of 0.56% and 0.75% are found for Re-Quinta-C12-Br (**G**) and Re-Pyta-C12-Cl (**M**), respectively, which matches values for complexes of similar structures under comparable conditions.[5b] The Taquin analogue **E** shows a quantum yield value of 1.30%, while the Tapy derivative **L** has a quantum yield of 3.56%, which represents roughly 2-fold and 4-fold increases, respectively

dx.doi.org/10.1021/ic5007007 | *Inorg. Chem.* 2014, 53, 6204−6223

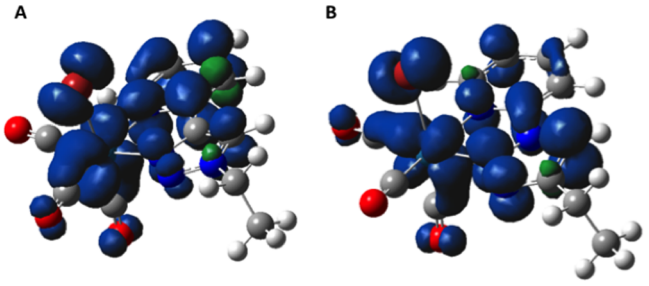

Figure 14. Spin density plots of the optimized triplet states for Re-Pyta-Br (A) and Re-Tapy-Br (B).

(Table 3). The results obtained for the Tapy complexes bearing long alkyl chains **J**−**L** are particularly interesting and, to the best of our knowledge, unprecedented for Re tricarbonyl complexes in aqueous medium. It is striking to obtain such an enhancement in the photophysical properties with such a small difference in the chemical structure of the complexes. From this point on, we focus on the complexes of the Tapy series, as this series displays by far the most interesting properties. We performed further studies in an attempt to rationalize our observations and determine whether the peculiar behavior revealed originates from intrinsic electronic properties of the Tapy core in the coordination sphere of the rhenium or from a particular conformational or aggregation state of the Re-Tapy complexes in aqueous solution.

Side Chain Effect and Luminescence Modulation. As stated above, modifications in the side chain cause profound changes in the emission intensities of the complexes of Taquin and Tapy series in aqueous solution in comparison to acetonitrile. We studied this behavior for the Tapy series in more detail, and results are presented thereafter.

In organic solvent, the photophysical properties of the complexes are identical (λ_{exc}, λ_{em}, Φ) (Figure 10, left). In aqueous solution, a small blue shift (6 nm) is observed in the maximum emission wavelength for the longer alkyl chain derivatives **J** and **K** (Figure 10, right). The quantum yields values of all complexes **H**−**K** increase from acetonitrile to water, but more importantly, the complexes **J** and **K** bearing long alkyl chains (from C8) show an impressive enhancement in emission and quantum yield (Figure 10 and Table 3) in water in comparison to **H** and **I**. This behavior was already reported for

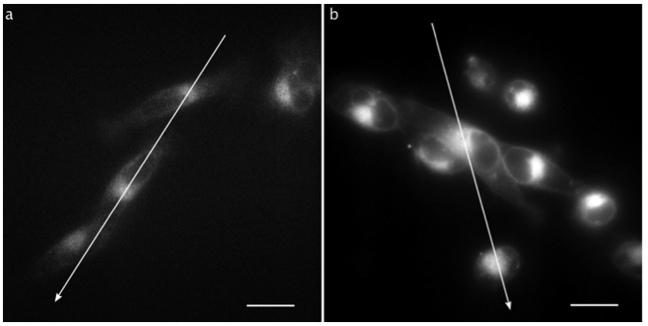

Figure 16. MDA-MB-231 cells (scale bars 20 μm). Luminescence signal for cells incubated at 25 μM at 37 °C for 1 h with (a) Re-Pyta-C12-Cl (**M**) and (b) Re-Tapy-C12-Cl (**L**). The same illumination and recording parameters were used for both images, but image (a) is presented with enhanced brightness/contrast conditions in order to see the cells. The intensity profiles shown in Figure 17 are measured along the white arrow for each image. All cells were fixed, and slides were mounted.

Pyta-based or 2,2′-bipyridine-based rhenium tricarbonyl complexes.[20] This effect of the side chains can be explained by a chain wrapping or fold back onto the luminescent Re core. In aqueous solution, the complex adopts a conformation driven by hydrophobic forces in which the alkyl chain wraps around the Re core and enhances its emission properties by isolating it from the solvent environment. As a result, the excited state is shielded from solvent quenching effect. This hypothesis is further supported by the results obtained from temperature studies[20b,c] (see the Supporting Information).

However, this side chain effect is not sufficient to explain the luminescence enhancement of the Tapy series in comparison to Pyta complexes. A strong emission enhancement is indeed observed for Tapy complexes for all of the side chains used. It is well exemplified by the fact that complex **I** shows a stronger emission in water than in acetonitrile, whereas the emission of the corresponding Pyta complex is totally quenched in aqueous medium.[20b] Tapy-based rhenium tricarbonyl complexes are thus intrinsically more luminescent than the corresponding Pyta complexes in both organic and aqueous media.

Pyta and Tapy complexes with C12 side chains and halides as ligands show the same solubility range as determined by UV titration experiments: 7.0 μM for complexes Re-Tapy-C12-Br

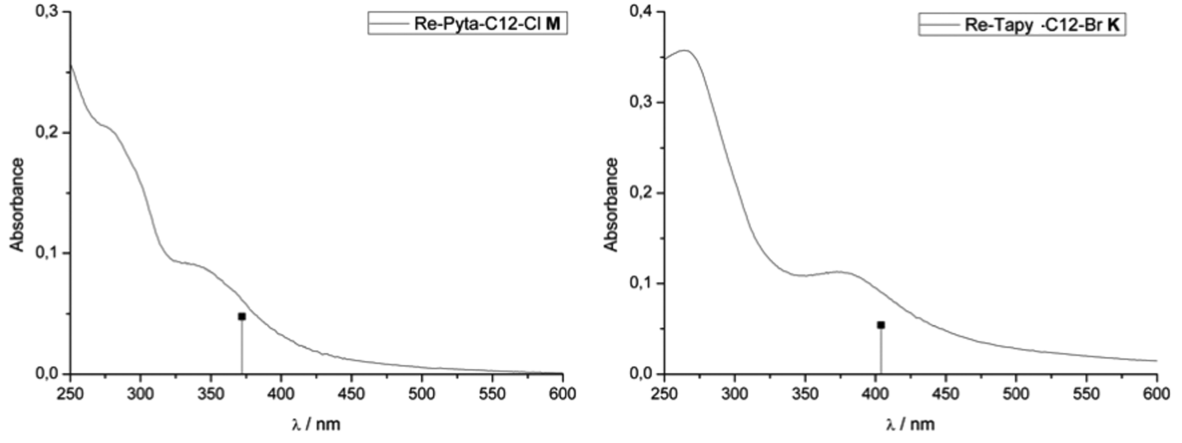

Figure 15. Absorption spectra (10 μM in H_2O/DMSO 98/2, 25 °C) and TD-DFT predicted transitions (vertical lines) for Re-Pyta-C12-Cl (**M**) (left) and Re-Tapy-C12-Br (**K**) (right).

dx.doi.org/10.1021/ic5007007 | *Inorg. Chem.* 2014, 53, 6204−6223

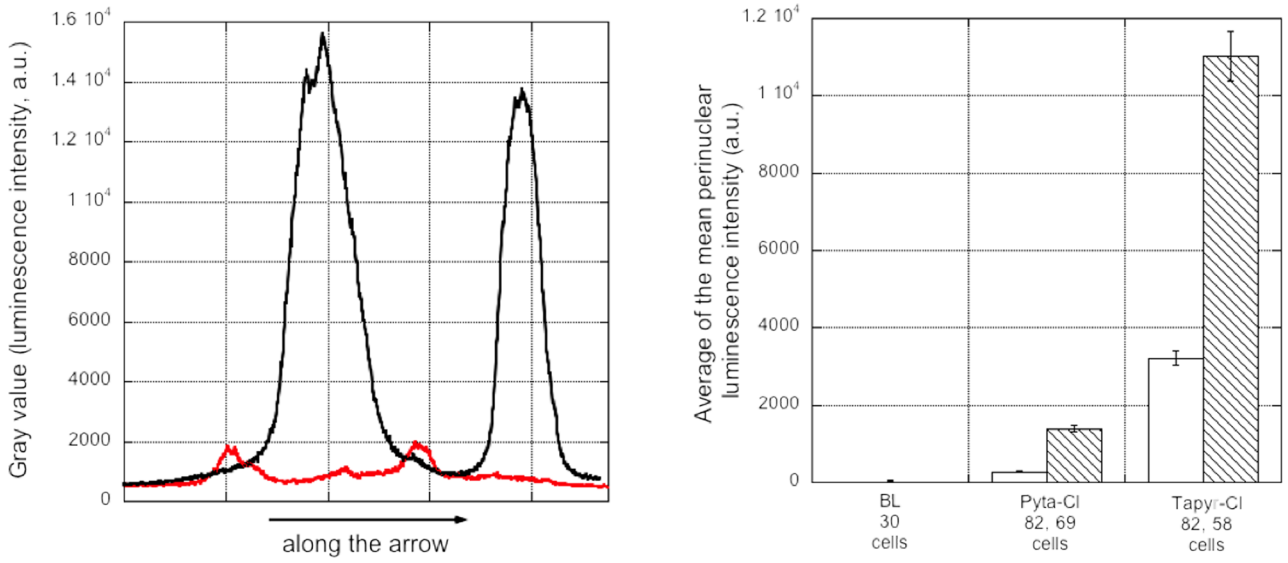

Figure 17. (left) Intensity profiles collected along the white arrow for each case in Figure 16 (performed with ImageJ software). The same illumination and recording parameters were used for both profiles. Cells were incubated at 25 μM at 37 °C for 1 h with Re-Pyta-C12-Cl (**M**; image a, red trace) and Re-Tapy-C12-Cl (**L**; image b, black trace). (right) Average of the mean perinuclear luminescence for collections of MDA-MB-231 control cells and cells incubated for 1 h at 37 °C at 10 μM (white bars) or 25 μM (dashed bars). For each condition the number of cells used is specified. Luminescence signals were monitored using the same filter set (see the Experimental Section) and the same conditions of acquisition. The mean perinuclear luminescence was corrected for the background before averaging. The standard error was calculated with a Student coefficient for a two-sided confidence interval of 95% and for the number of cells of the collection.

(**K**) and Re-Tapy-C12-Cl (**L**) and 6.0 μM for Re-Pyta-C12-Cl (**M**) in a H_2O/DMSO 98/2 mixture. This is indicative of a similar state in aqueous solutions at identical concentrations, and therefore a different aggregation state could not account for the difference in luminescence intensity observed.

Ligand Exchange and Stability: Conductivity and NMR Studies. To further compare the Pyta and Tapy complexes, we explored their stability and potential ligand exchange in polar coordinating solvents. It has indeed been described by means of conductivity measurements that the bromide ligand in other Pyta and Quinta complexes is immediately exchanged for water under aqueous conditions.[5b,22] We therefore performed conductivity measurements of 10 μM solutions of complexes Re-Tapy-C12-Br (**K**), Re-Tapy-C12-Cl (**L**), and Re-Pyta-C12-Cl (**M**) in 5% DMSO/H_2O to investigate this halide ligand exchange. The conductivity measurements were performed over a 24 h period and compared with identical concentrations of NaCl (10.88 μS cm^{-1}) and $CaCl_2$ (23.63 μS cm^{-1}) in the same solvent mixture. In all cases, over 24 h, the rhenium complexes exhibit stable conductivity values lower than that of the 1/1 electrolyte (4.77, 3.04, and 2.98 μS cm^{-1} for Re-Tapy-C12-Br (**K**), Re-Tapy-C12-Cl (**L**), and Re-Pyta-C12-Cl (**M**), respectively). This reflects that no halide for H_2O exchange occurs for these three complexes at the low concentrations used.

DMSO is often used as an additive in solutions for such complexes to enable their solubility in aqueous media, and stock solutions in DMSO are frequently used for biological experiments. A fast ligand dissociation has been recently reported in DMSO solutions of Ru(η^6-arene)Cl_2(L).[23] We therefore recorded ^{1}H NMR spectra of complex **M** and complexes **K** and **L** along with their ligand alone **17** in d_6-DMSO (ca. 2.0 mg in 0.4 mL) at different time intervals. The results obtained after 4 days at room temperature are shown in Figure 11.

This study highlights an interesting difference in the stability of Pyta and Tapy complexes in these conditions. No ligand dissociation is observed after 4 days for Re-Pyta-C12-Cl (**M**), which shows only one set of signals in ^{1}H NMR (Figure 11). However, a slow and partial dissociation of approximately 30% is evidenced for Tapy complexes **K** and **L** under the same conditions (no dissociation is observed over 20 h). Two sets of signals in the ^{1}H spectra are indeed visible corresponding to the rhenium complex and to the ligand alone, as highlighted in Figure 11 in the stacked spectra. An equilibrium between coordinated and uncoordinated ligand is slowly established as the percentage of dissociation reaches a maximum between 36 and 40% and does not increase any more. The decoordination of rhenium could arise from a stronger destabilization of the halide ligand by the trans effect of the carbonyl ligand in the Tapy complexes in comparison with the Pyta complexes. The higher stability of the Pyta complex under these conditions is also in agreement with a higher electron density on the N(3) of the triazole in comparison with the coordinating N(2) in the Tapy ligand (Mülliken population analysis charges from DFT calculations (vide infra): Tapy complex, N(2) −0.166; Pyta complex, N(3) −0.431).[24] As a result of the partial decoordination of the Tapy complexes in concentrated DMSO solutions, solutions have to be freshly prepared immediately before use for photophysical or biological studies.

Theoretical Studies. DFT calculations were performed to compare the geometric and electronic structures of the Re-Pyta and Re-Tapy complexes. The results obtained for Re-Pyta are consistent with the already reported calculations on other Re-Pyta complexes bearing a halide or a water molecule in their coordination sphere.[5b,f] We limited the alkyl chain length to an ethyl group to reduce calculation time. We used the B3LYP functional in combination with the LANL2DZ basis set for rhenium and 6-311G** basis set for all other atoms.[25]

In the singlet optimized structures of Re-Pyta-Br and Re-Tapy-Br, the Pyta and Tapy ligands were found to be planar. The predicted Re−CO bond lengths are similar for both complexes (1.917−1.935 Å). The Re−halide bonds are longer than the Re−CO bonds, with predicted values of 2.678 and

dx.doi.org/10.1021/ic5007007 | Inorg. Chem. 2014, 53, 6204−6223

2.675 Å for Re−Br bonds in Re-Pyta and Re-Tapy, respectively. The Re−Cl bonds in the corresponding complexes are slightly shorter and are calculated to be 2.533 and 2.530 Å, respectively. The distances Re−N(py) (2.241 vs 2.226 Å) and Re−N(ta) (2.179 vs 2.168 Å) are slightly shorter in the Re-Tapy complex. This could be due to the shorter length of the bond constituting the bridge between the pyridine and the triazole ring in the Tapy ligand (C−N bond 1.406 Å vs C−C bond 1.454 Å in the pyta ligand). The dihedral angles between the ligand and the $Re(CO)_2$ equatorial unit are similar in both cases, with calculated values of 9.4 and 10.4° for Re-Pyta and Re-Tapy, respectively.

Frontier orbital diagrams are shown in Figures 12 and 13, respectively. As already described for Re-Pyta complexes, the HOMO-4 to HOMO levels are rhenium-based with partial carbonyl character and a bromide component except for HOMO-2.[5b,f] These features are similarly found in the Re-Tapy complex, for which the only difference is a higher contribution of the ligand in HOMO-3. In both cases, the HOMO and HOMO-1 levels are close in energy. The HOMO and HOMO-1 levels contain significant rhenium $5d_{xz}$ and $5d_{yz}$ character, while the HOMO-2 level contains the $5d_{xy}$ orbital. The LUMO and LUMO+1 levels are mainly centered on the aromatic ligand and particularly the π^* antibonding orbital. These results are fully consistent with previously published studies on Re-Pyta complexes and show strong similarities in the molecular orbital diagrams of Pyta- and Tapy-based complexes. The Re-Tapy complex is characterized by orbitals of lower energies and a smaller gap (2.88 eV vs 3.06 eV), which is in good agreement with the values obtained experimentally by UV−vis absorption (3.08 eV for **K** and 3.28 eV for **M**).

We calculated and compared the spin densities of the optimized triplet electronic states of Re-Pyta and Re-Tapy complexes. The spin density plots, shown in Figure 14, support the MLCT character of the optimized triplet state. The spin densities on rhenium are comparable for both complexes, but a difference in their distribution on the ligands is observed. The spin density is stronger on the pyridine ring in the Pyta ligand, whereas it is more localized on the triazole ring in the Tapy ligand. This difference in spin density distribution on the ligand in the optimized triplet state could account for the variation in the luminescence observed in the corresponding complexes.

We finally compared the nature of the electronic transitions for Re-Pyta[5b,f] and Re-Tapy complexes using time-dependent DFT calculations. The UB3LYP/LANL2DZ/6-311G** level was used with a polarized continuum model for water. The lowest-energy transitions are summarized in the Supporting Information (6 for the Re-Pyta complex and 20 for the Re-Tapy complex; Tables S3 and S4 in the Supporting Information, respectively). The lowest energy transitions with significant oscillator strength are shown along with the experimental absorption spectra in Figure 15. The predicted lowest energy transition for Re-Pyta-Br at 372 nm (f = 0.095) is a transition from the metal-based HOMO-1 orbital to the LUMO antibonding ligand-based orbital, thus constituting a MLCT band. In the case of Re-Tapy-Br, similarly, the predicted lowest energy transition at 404 nm (f = 0.1083) is a transition from a combination of the metal-based HOMO and HOMO-1 orbitals to the LUMO π^* orbital and is also of MLCT character. The two transitions at 310 nm (f = 0.0793) and 302 nm (f = 0.0788) are from HOMO-3 and HOMO-4, respectively, to the LUMO showing an additional intraligand transition character.

The theoretical calculations reproduce satisfactorily the experimental data obtained by UV for both Re-Pyta and Re-Tapy complexes. A variation in the spin density distribution on the ligands is observed in the optimized triplet states, which suggests a difference in the emissive state in Re-Pyta and Re-Tapy complexes, respectively, that could account for the variation in the luminescence observed.

Preliminary Cellular Imaging. We finally performed preliminary cellular imaging studies in MDA-MB-231 breast cancer cells and compared luminescence signals for Re-Tapy-C12-Cl (**L**) and Re-Pyta-C12-Cl (**M**). The compounds were incubated at 10 or 25 μM for 1 h; the cells were subsequently fixed (PFA) and imaged after the slides were mounted. As shown in Figure 16, both complexes show similar perinuclear distributions, as already described for closely related complexes under the same conditions.[6,20b] In contrast, the luminescence intensity is tremendously enhanced in the case of Re-Tapy-C12-Cl (**L**), as illustrated by the intensity profiles recorded along cells presented in Figure 17 (left) or by the average intensity of the mean perinuclear luminescence obtained for collections of MDA-MB-231 cells incubated with complexes shown in Figure 17 (right). A difference in cellular uptake is unlikely, given the high similarity in the chemical structure and hence lipophilicity of both complexes. This luminescence enhancement can be explained by the improved photophysical properties of the Re-Tapy complexes as described above.

CONCLUSION

New rhenium tricarbonyl complexes prepared from different bidentate aromatic ligands were developed. Complexes with benzothiadiazole−triazole ligands show interesting luminescent quantum yields in acetonitrile and may constitute valuable luminescent metal complexes in organic media. A series of complexes with bidentate 1-(2-quinolinyl)-1,2,3-triazole (Taquin) and 1-(2-pyridyl)-1,2,3-triazole (Tapy) ligands bearing various 4-substituted alkyl side chains has been designed and synthesized with efficient procedures. Their photophysical properties have been characterized in acetonitrile and in a H_2O/DMSO (98/2) mixture and compared with those of the parent Quinta- and Pyta-based complexes. Tapy complexes bearing long alkyl chains show impressive enhancement of their luminescent properties in aqueous medium relative to the parent Pyta complex. Stability studies in coordinating DMSO highlight a partial decoordination in the case of the Tapy complex. Theoretical calculations have been performed to further characterize this new class of rhenium tricarbonyl. Preliminary cellular imaging studies in MDA-MB231 breast cancer cells reveal a strong increase in the luminescence signal in cells incubated with the Tapy complex. We demonstrated how tiny structural modifications can cause profound changes in the photophysical properties of such metal complexes. Further experiments are needed to rationalize this behavior. This study nevertheless points out the potential of the Tapy ligand in coordination chemistry, which has been so far underexploited.

ASSOCIATED CONTENT

Supporting Information

Text, tables, a figure, and a CIF file giving crystallographic data and refinement details and experimental bond lengths and angles for complex **F**, predicted transitions, and temperature studies. This material is available free of charge via the Internet at http://pubs.acs.org.

dx.doi.org/10.1021/ic5007007 | Inorg. Chem. 2014, 53, 6204−6223

AUTHOR INFORMATION

Corresponding Author

*E-mail for H.C.B.: helene.bertrand@ens.fr.

Notes

The authors declare no competing financial interest.

ACKNOWLEDGMENTS

The ENS is acknowledged for a Ph.D. fellowship for S.C.. Dr. A. Vessières is gratefully acknowledged for cell culture facilities and Dr. Z. Gueroui for access to the fluorescence microscope.

REFERENCES

(1) (a) Demas, J. N.; DeGraff, B. A. Design and Applications of Highly Luminescent Transition Metal Complexes. In *Topics in Fluorescence Spectroscopy*; Lakowicz, J. R., Ed.; Springer: Berlin, 1994; Vol. *4* (Probe Design and Chemical Sensing). (b) Thorp-Greenwood, F. L. *Organometallics* **2012**, *31* (16), 5686−5692.

(2) (a) Lo, K. K.-W.; Louie, M.-W.; Zhang, K. Y. *Coord. Chem. Rev.* **2010**, *254* (21−22), 2603−2622. (b) Lo, K. K.-W.; Tsang, K. H.-K.; Sze, K.-S.; Chung, C.-K.; Lee, T. K.-M.; Zhang, K. Y.; Hui, W.-K.; Li, C.-K.; Lau, J. S.-Y.; Ng, D. C.-M.; Zhu, N. *Coord. Chem. Rev.* **2007**, *251* (17−20), 2292−2310.

(3) (a) Baggaley, E.; Weinstein, J. A.; Williams, J. A. G. *Coord. Chem. Rev.* **2012**, *256* (15−16), 1762−1785. (b) Balasingham, R. G.; Coogan, M. P.; Thorp-Greenwood, F. L. *Dalton Trans.* **2011**, *40* (44), 11663−11674. (c) Butler, I. S.; Kengne-Momo, R. P.; Jaouen, G.; Policar, C.; Vessieres, A. *Appl. Spectrosc. Rev.* **2012**, *47* (7), 531−549. (d) Fernandez-Moreira, V.; Thorp-Greenwood, F. L.; Coogan, M. P. *Chem. Commun.* **2010**, *46* (2), 186−202. (e) Lo, K. K.-W.; Choi, A. W.-T.; Law, W. H.-T. *Dalton Trans.* **2012**, *41* (20), 6021−6047. (f) Lo, K. K.-W.; Zhang, K. Y.; Li, S. P.-Y. *Eur. J. Inorg. Chem.* **2011**, *2011* (24), 3551−3568. (g) Louie, M.-W.; Choi, A. W.-T.; Liu, H.-W.; Chan, B. T.-N.; Lo, K. K.-W. *Organometallics* **2012**, *31* (16), 5844−5855. (h) Sacksteder, L.; Zipp, A. P.; Brown, E. A.; Streich, J.; Demas, J. N.; DeGraff, B. A. *Inorg. Chem.* **1990**, *29* (21), 4335−4340. (i) Thorp-Greenwood, F. L.; Coogan, M. P.; Hallett, A. J.; Laye, R. H.; Pope, S. J. A. *J. Organomet. Chem.* **2009**, *694* (9−10), 1400−1406.

(4) (a) Anderson, C. B.; Elliott, A. B. S.; Lewis, J. E. M.; McAdam, C. J.; Gordon, K. C.; Crowley, J. D. *Dalton Trans.* **2012**, *41* (48), 14625−14632. (b) Bartholoma, M.; Valliant, J.; Maresca, K. P.; Babich, J.; Zubieta, J. *Chem. Commun.* **2009**, No. 5, 493−512. (c) Wei, L.; Babich, J. W.; Ouellette, W.; Zubieta, J. *Inorg. Chem.* **2006**, *45* (7), 3057−3066. (d) Wrighton, M.; Morse, D. L. *J. Am. Chem. Soc.* **1974**, *96* (4), 998−1003.

(5) (a) Bullock, S.; Hallett, A. J.; Harding, L. P.; Higginson, J. J.; Piela, S. A. F.; Pope, S. J. A.; Rice, C. R. *Dalton Trans.* **2012**, *41* (48), 14690−14696. (b) Huang, R.; Langille, G.; Gill, R. K.; Li, C. M. J.; Mikata, Y.; Wong, M. Q.; Yapp, D. T.; Storr, T. *J. Biol. Inorg. Chem.* **2013**, *18* (7), 831−844. (c) Kim, T. Y.; Elliott, A. B. S.; Shaffer, K. J.; John McAdam, C.; Gordon, K. C.; Crowley, J. D. *Polyhedron* **2013**, *52* (0), 1391−1398. (d) Obata, M.; Kitamura, A.; Mori, A.; Kameyama, C.; Czaplewska, J. A.; Tanaka, R.; Kinoshita, I.; Kusumoto, T.; Hashimoto, H.; Harada, M.; Mikata, Y.; Funabiki, T.; Yano, S. *Dalton Trans.* **2008**, No. 25, 3292−3300. (e) Seridi, A.; Wolff, M.; Boulay, A.; Saffon, N.; Coulais, Y.; Picard, C.; Machura, B.; Benoist, E. *Inorg. Chem. Commun.* **2011**, *14* (1), 238−242. (f) Wolff, M.; Munoz, L.; Francois, A.; Carrayon, C.; Seridi, A.; Saffon, N.; Picard, C.; Machura, B.; Benoist, E. *Dalton Trans.* **2013**, *42* (19), 7019−7031.

(6) Clede, S.; Lambert, F.; Sandt, C.; Gueroui, Z.; Refregiers, M.; Plamont, M. A.; Dumas, P.; Vessieres, A.; Policar, C. *Chem. Commun.* **2012**, *48* (62), 7729−7731.

(7) Clede, S.; Lambert, F.; Sandt, C.; Kascakova, S.; Unger, M.; Harte, E.; Plamont, M. A.; Saint-Fort, R.; Deniset-Besseau, A.; Gueroui, Z.; Hirschmugl, C.; Lecomte, S.; Dazzi, A.; Vessieres, A.; Policar, C. *Analyst* **2013**, *138* (19), 5627−5638.

(8) Chattopadhyay, B.; Vera, C. I. R.; Chuprakov, S.; Gevorgyan, V. *Org. Lett.* **2010**, *12* (9), 2166−2169.

(9) Rodriguez, J. G.; de los Rios, C.; Lafuente, A. *Tetrahedron* **2005**, *61* (38), 9042−9051.

(10) Kvaskoff, D.; Vosswinkel, M.; Wentrup, C. *J. Am. Chem. Soc.* **2011**, *133* (14), 5413−5424.

(11) Keith, J. M. *J. Org. Chem.* **2006**, *71* (25), 9540−9543.

(12) Chang, S.; Lee, M.; Jung, D. Y.; Yoo, E. J.; Cho, S. H.; Han, S. K. *J. Am. Chem. Soc.* **2006**, *128* (38), 12366−12367.

(13) Katagiri, T.; Tsurugi, H.; Satoh, T.; Miura, M. *Chem. Commun.* **2008**, No. 29, 3405−3407.

(14) (a) Shaikh, T. M.; Sudalai, A. *Eur. J. Org. Chem.* **2010**, *2010* (18), 3437−3444. (b) Juricek, M.; Kouwer, P. H. J.; Rehak, J.; Sly, J.; Rowan, A. E. *J. Org. Chem.* **2009**, *74* (1), 21−25.

(15) Bijleveld, J. C.; Shahid, M.; Gilot, J.; Wlenk, M. M.; Janssen, R. A. J. *Adv. Funct. Mater.* **2009**, *19* (20), 3262−3270.

(16) Maisonneuve, S.; Fang, Q.; Xie, J. *Tetrahedron* **2008**, *64* (37), 8716−8720.

(17) (a) Sheldrick, G. M. *SHELXS-97, Program for Crystal Structure Solution*; University of Göttingen, Göttingen, Germany, 1997. (b) Sheldrick, G. M. *SHELXL-97, Program for the Refinement of Crystal Structures from Diffraction Data*; University of Göttingen, Göttingen, Germany, 1997. (c) Farrugia, L. J. *J. Appl. Crystallogr.* **1999**, *32*, 837−838.

(18) Ellanki, A. R.; Islam, A.; Rama, V. S.; Pulipati, R. P.; Rambabu, D.; Rama Krishna, G.; Malla Reddy, C.; Mukkanti, K.; Vanaja, G. R.; Kalle, A. M.; Shiva Kumar, K.; Pal, M. *Bioorg. Med. Chem. Lett.* **2012**, *22* (10), 3455−3459.

(19) (a) Gu, S.; Xu, H.; Zhang, N.; Chen, W. *Chem. Asian J.* **2010**, *5* (7), 1677−1686. (b) Stengel, I.; Mishra, A.; Pootrakulchote, N.; Moon, S.-J.; Zakeeruddin, S. M.; Gratzel, M.; Bauerle, P. *J. Mater. Chem.* **2011**, *21* (11), 3726−3734.

(20) (a) Choi, A. W.-T.; Louie, M.-W.; Li, S. P.-Y.; Liu, H.-W.; Chan, B. T.-N.; Lam, T. C.-Y.; Lin, A. C.-C.; Cheng, S.-H.; Lo, K. K.-W. *Inorg. Chem.* **2012**, *51* (24), 13289−13302. (b) Clede, S.; Lambert, F.; Saint-Fort, R.; Plamont, M.-A.; Bertrand, H.; Vessières, A.; Policar, C. *Chem. Eur. J.*, DOI: 10.1002/chem.201402471. (c) Coogan, M. P.; Fernandez-Moreira, V.; Hess, J. B.; Pope, S. J. A.; Williams, C. *New J. Chem.* **2009**, *33* (5), 1094−1099. (d) Reitz, G. A.; Demas, J. N.; DeGraff, B. A.; Stephens, E. M. *J. Am. Chem. Soc.* **1988**, *110* (15), 5051−5059. (e) Sacksteder, L.; Lee, M.; Demas, J. N.; DeGraff, B. A. *J. Am. Chem. Soc.* **1993**, *115* (18), 8230−8238.

(21) (a) Garcia, L.; Lazzaretti, M.; Diguet, A.; Mussi, F.; Bisceglie, F.; Xie, J.; Pelosi, G.; Buschini, A.; Baigl, D.; Policar, C. *New J. Chem.* **2013**, *37* (10), 3030−3034. (b) Garcia, L.; Maisonneuve, S.; Marcu, J. O. S.; Guillot, R.; Lambert, F.; Xie, J.; Policar, C. *Inorg. Chem.* **2011**, *50* (22), 11353−11362.

(22) Storr, T.; Obata, M.; Fisher, C. L.; Bayly, S. R.; Green, D. E.; Brudziñska, I.; Mikata, Y.; Patrick, B. O.; Adam, M. J.; Yano, S.; Orvig, C. *Chem. Eur. J.* **2005**, *11* (1), 195−203.

(23) Patra, M.; Joshi, T.; Pierroz, V.; Ingram, K.; Kaiser, M.; Ferrari, S.; Spingler, B.; Keiser, J.; Gasser, G. *Chem. Eur. J.* **2013**, *19* (44), 14768−14772.

(24) Schulze, B.; Schubert, U. S. *Chem. Soc. Rev.* **2014**, *43*, 2522−2571.

(25) Frisch, M. J.; Trucks, G. W.; Schlegel, H. B.; Scuseria, G. E.; Robb, M. A.; Cheeseman, J. R.; Scalmani, G.; Barone, V.; Mennucci, B.; Petersson, G. A.; Nakatsuji, H.; Caricato, M.; Li, X.; Hratchian, H. P.; Izmaylov, A. F.; Bloino, J.; Zheng, G.; Sonnenberg, J. L.; Hada, M.; Ehara, M.; Toyota, K.; Fukuda, R.; Hasegawa, J.; Ishida, M.; Nakajima, T.; Honda, Y.; Kitao, O.; Nakai, H.; Vreven, T.; Montgomery, J. A., Jr.; Peralta, J. E.; Ogliaro, F.; Bearpark, M.; Heyd, J. J.; Brothers, E.; Kudin, K. N.; Staroverov, V. N.; Kobayashi, R.; Normand, J.; Raghavachari, K.; Rendell, A.; Burant, J. C.; Iyengar, S. S.; Tomasi, J.; Cossi, M.; Rega, N.; Millam, J. M.; Klene, M.; Knox, J. E.; Cross, J. B.; Bakken, V.; Adamo, C.; Jaramillo, J.; Gomperts, R.; Stratmann, R. E.; Yazyev, O.; Austin, A. J.; Cammi, R.; Pomelli, C.; Ochterski, J. W.; Martin, R. L.; Morokuma, K.; Zakrzewski, V. G.; Voth, G. A.; Salvador, P.; Dannenberg, J. J.; Dapprich, S.; Daniels, A. D.; Farkas, O.; Foresman, J. B.; Ortiz, J. V.; Cioslowski, J.; Fox, D. J. *Gaussian 09*; Gaussian, Inc., Wallingford, CT, 2009.